

AD-A034 055

ANALYTIC SCIENCES CORP READING MASS
EFFICIENT ESTIMATION TECHNIQUES FOR INTEGRATED GRAVITY DATA PRO--ETC(U)

F/G 8/E

SEP 76 S W THOMAS, W G HELLER

F19628-76-C-0014

UNCLASSIFIED

TASC-TR-680-1

AFGL-TR-76-0232

NL

1 OF 1
AD-A
034 055



END
DATE
FILMED
2-15-77
NTIS

U.S. DEPARTMENT OF COMMERCE
National Technical Information Service

AD-A034 055

EFFICIENT ESTIMATION TECHNIQUES FOR
INTEGRATED GRAVITY DATA PROCESSING

ANALYTIC SCIENCES CORPORATION
READING, PENNSYLVANIA

30 SEPTEMBER 1976

011101

AFGL-TR-76-0232



EFFICIENT ESTIMATION TECHNIQUES FOR INTEGRATED GRAVITY DATA PROCESSING

Stephen W. Thomas
Warren G. Heller

The Analytic Sciences Corporation
Six Jacob Way
Reading, Massachusetts 01867

30 September 1976

Final Report
15 August 1975 - 31 July 1976



Approved for Public Release; Distribution Unlimited

AIR FORCE GEOPHYSICS LABORATORY
AIR FORCE SYSTEMS COMMAND
UNITED STATES AIR FORCE
Hanscom AFB, Massachusetts 01731

REPRODUCED BY
NATIONAL TECHNICAL
INFORMATION SERVICE
U. S. DEPARTMENT OF COMMERCE
SPRINGFIELD, VA 22161

ADA034055

Qualified requestors may obtain additional copies from the Defense Documentation Center. All others should apply to the National Technical Information Service.

UNCLASSIFIED

SECURITY CLASSIFICATION OF THIS PAGE (When Data Entered)

REPORT DOCUMENTATION PAGE		READ INSTRUCTIONS BEFORE COMPLETING FORM
1. REPORT NUMBER AFGL-TR-76-0232	2. GOVT ACCESSION NO. none	3. RECIPIENT'S CATALOG NUMBER
4. TITLE (and Subtitle) Efficient Estimation Techniques for Integrated Gravity Data Processing		5. TYPE OF REPORT & PERIOD COVERED Final 8/15/75 - 7/31/76
		6. PERFORMING ORG. REPORT NUMBER TR-680-1
7. AUTHOR(s) Stephen W. Thomas Warren G. Heller		8. CONTRACT OR GRANT NUMBER(s) F19628-76-C-0014
9. PERFORMING ORGANIZATION NAME AND ADDRESS The Analytic Sciences Corporation Six Jacob Way Reading, Massachusetts 01867		10. PROGRAM ELEMENT, PROJECT, TASK AREA & WORK UNIT NUMBERS 62101F 76000301
11. CONTROLLING OFFICE NAME AND ADDRESS Air Force Geophysics Laboratory Hanscom AFB, Massachusetts 1731 Monitor/George Hadgigeorge/LWG		12. REPORT DATE 30 September 1976
		13. NUMBER OF PAGES 77
14. MONITORING AGENCY NAME & ADDRESS (if different from Controlling Office)		15. SECURITY CLASS. (of this report) UNCLASSIFIED
		15a. DECLASSIFICATION/DOWNGRADING SCHEDULE
16. DISTRIBUTION STATEMENT (of this Report) Approved for Public Release - Distribution Unlimited		
17. DISTRIBUTION STATEMENT (of the abstract entered in Block 20, if different from Report)		
18. SUPPLEMENTARY NOTES		
19. KEY WORDS (Continue on reverse side if necessary and identify by block number) Gravity Disturbance, Least-squares Estimation, Multisensor, Frequency Domain, Efficient Computation		
20. ABSTRACT (Continue on reverse side if necessary and identify by block number) A mathematical technique is developed for the combined use of various types of gravimetric data in the estimation of such gravity quantities as the disturbance potential and the gravity disturbance vector. Modern frequency domain techniques are introduced which substantially reduce the computer process- ing requirements associated with least-squares gravity quantity estimation. This approach represents an extension of existing		

SECURITY CLASSIFICATION OF THIS PAGE(When Data Entered)

BY _____
FBI MEMPHIS OFFICE

DATE	TIME	AL.
A		

SECURITY CLASSIFICATION OF THIS PAGE(When Data Entered)

TABLE OF CONTENTS

	<u>Page No.</u>
List of Figures	iv
List of Tables	v
1. INTRODUCTION	1-1
1.1 Background and Purpose	1-1
1.2 Scope	1-3
1.3 Technical Approach	1-5
1.4 Overview	1-8
2. LEAST SQUARES ESTIMATION OF GRAVITY QUANTITIES	2-1
2.1 Statement of the Problem	2-1
2.1.1 Example Problem Formulation	2-2
2.1.2 The Role of Statistical Models	2-4
2.2 Least-Squares Estimation and Error Analysis	2-5
2.3 Statistical Gravity Models	2-8
3. FREQUENCY DOMAIN ESTIMATION WITH SINGLE-SENSOR DATA	3-1
3.1 The Frequency Domain Algorithm	3-1
3.2 Relationship With Least-Squares Estimation	3-4
3.3 Numerical Simulation	3-9
3.4 Edge Effect Analysis	3-15
4. MULTISENSOR FREQUENCY DOMAIN ESTIMATION	4-1
4.1 Problem Formulation	4-1
4.2 Sequential, Sensor-By-Sensor Estimation	4-3
4.3 Sensor-By-Sensor Estimation in the Frequency Domain	4-6
4.4 Multisensor Numerical Simulation	4-11
5. CONCLUSIONS AND RECOMMENDATIONS	5-1
APPENDIX A - ASYMPTOTIC OPTIMALITY OF FINITE, FREQUENCY DOMAIN ESTIMATION	A-1
APPENDIX B - MULTISENSOR, DISCRETE WIENER FILTERING	B-1
APPENDIX C - DERIVATION OF FREQUENCY DOMAIN STATISTICS USING THE SAMPLING THEOREM	C-1
REFERENCES	R-1

LIST OF FIGURES

<u>Figure No.</u>		<u>Page No.</u>
1.1-1	Integrated Multisensor Gravity Data Processing	1-2
1.2-1	One-Dimensional, Multisensor Gravity Survey	1-4
1.3-1	Least Squares Estimation and Covariance Analysis	1-6
1.3-2	Relationships Between Direct Least-Squares Estimation and the Frequency Domain Approach	1-7
2.3-1	Geometry of Round Earth, Attenuated White Noise Model	2-10
3.1-1	Single Sensor Frequency Domain Estimation	3-3
3.2-1	The Generalized Wiener Filter	3-7
3.3-1	Projected Gravity Anomaly Estimation Error for an Airborne Survey With Gradiometry Only	3-12
3.3-2	Power Spectra for Airborne Gradiometry	3-13
3.3-3	Gravity-Anomaly/Gravity-Gradient Spectral Coherency Functions for Airborne Gradiometry	3-14
3.4-1	Estimation Error Sensitivity to Edge Effects	3-17
4.3-1	Sensor-By-Sensor Frequency Domain Estimation	4-8
4.3-2	Sampling Theorem for Finite Transforms	4-9
4.4-1	Projected Gravity Anomaly Estimation Error for a Combined Gradiometric/Gravimetric Survey	4-13

LIST OF TABLES

<u>Table No.</u>		<u>Page No.</u>
2.2-1	Vector Notation for Multisensor Estimation	2-5
3.1-1	Comparative Computer Processing Times for Direct, Least Squares Estimation and Frequency Domain Estimation	3-2
4.4-1	Projected Multisensor Gravity Survey Accuracies	4-14

1.

INTRODUCTION

1.1 BACKGROUND AND PURPOSE

Corresponding to the need for more accurate navigation and guidance systems, there has been an increasing interest in detailed knowledge of the Earth's gravity field. This interest has led to the development of new, sophisticated sensor technology to augment the more traditional gravimetric and astrogeodetic techniques. For example, SEASAT-A will soon be in orbit providing highly accurate over-ocean measurements of the undulation of the geoid. Similarly, gravity gradiometers capable of providing high quality data from a moving-vehicle survey are now under development. Satellite-to-satellite tracking techniques are another potential data source. Thus, large amounts of "multisensor gravity data" will be available in the near future.

The efficient use of abundant multisensor gravity data presents new problems in data processing and analysis. Navigation and guidance systems respond to many different gravity disturbance wavelengths, depending on factors such as vehicle speed and inertial navigation system (Schuler frequency) time constants. The various sensors offer differing spectral sensitivities to the disturbances in the Earth's gravity field. Gravity gradient data best describe the high frequency, fine-grained components of the gravity disturbance. Satellite altimetry and satellite-to-satellite tracking techniques are most responsive to lower frequency, regional gravity features. Conventional gravimetry provides still

another data source with an intermediate spectral response. To develop a complete, useful description of the Earth's gravity field requires the integrated processing of data from these and other sensors (Fig. 1.1-1). Efficient methods for the solution of this multisensor, gravity data processing problem are described in this report.

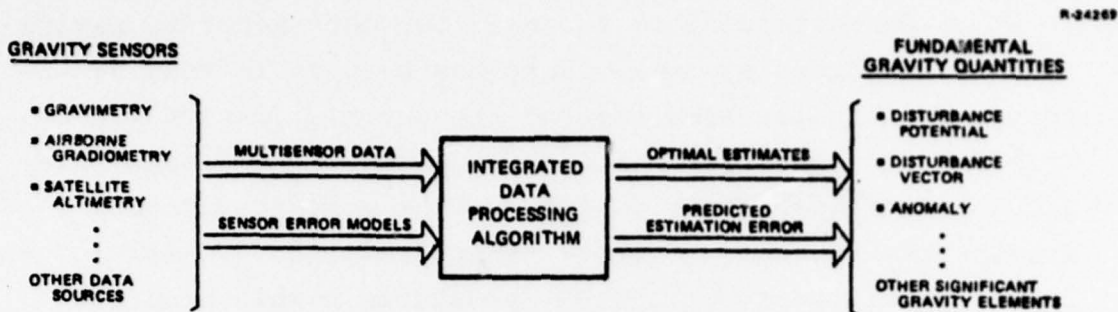


Figure 1.1-1 Integrated Multisensor Gravity Data Processing

This report extends the earlier work by TASC and others on gravity data processing by statistical least-squares techniques (Refs. 1-5). The least-squares approach has certain advantages. Given appropriate statistical gravity models, this methodology provides the means to compute optimal gravity quantity estimates based on data of quite general types. The accompanying capability for statistical estimation error analysis provides the method with a second attractive feature. Of course, the problem of obtaining and verifying the necessary statistical gravity models is not a trivial one. While not a major theme in this report, research in this important problem area is continuing (Refs. 6-11).

Given the availability of appropriate statistical models, the key issue in least-squares processing of multisensor gravity data is the development of techniques to

mitigate severe computer processing requirements. Even for amounts of data which are of moderate size for typical gravity applications, severe computer time requirements and associated numerical inaccuracies make the method extremely unattractive. Computational efficiency must be an inherent part of a practical gravity data processing algorithm. This report describes a technique which provides a substantial reduction in the computational cost of the least-squares methods as applied to gravity estimation.

1.2 SCOPE

This report is concerned with the development of mathematical techniques for the estimation of certain gravity quantities from sensors which are currently available, or which may be available, in the near future. The method developed here are appropriate for a broad range of gravity data sources, such as gravity gradiometry, satellite altimetry, gravimetry, and satellite-to-satellite tracking. The estimation methods of this report are constructed under the assumption that multisensor data is available on one-dimensional tracks, although the approach used here is applicable to more general survey geometries. The altitudes of the data tracks corresponding to different sensors may differ, as may the altitude of the survey track along which estimates are to be computed. Numerical results are specifically presented for gradiometry, gravimetry, and satellite altimetry. Typical quantities for which estimates are of interest are gravity disturbance potential and gravity anomaly. The gravity survey configuration treated in this report is depicted schematically in Fig. 1.2-1. The problem under consideration is to obtain efficient gravity quantity estimates based on moderate-to-large amounts of multisensor data.

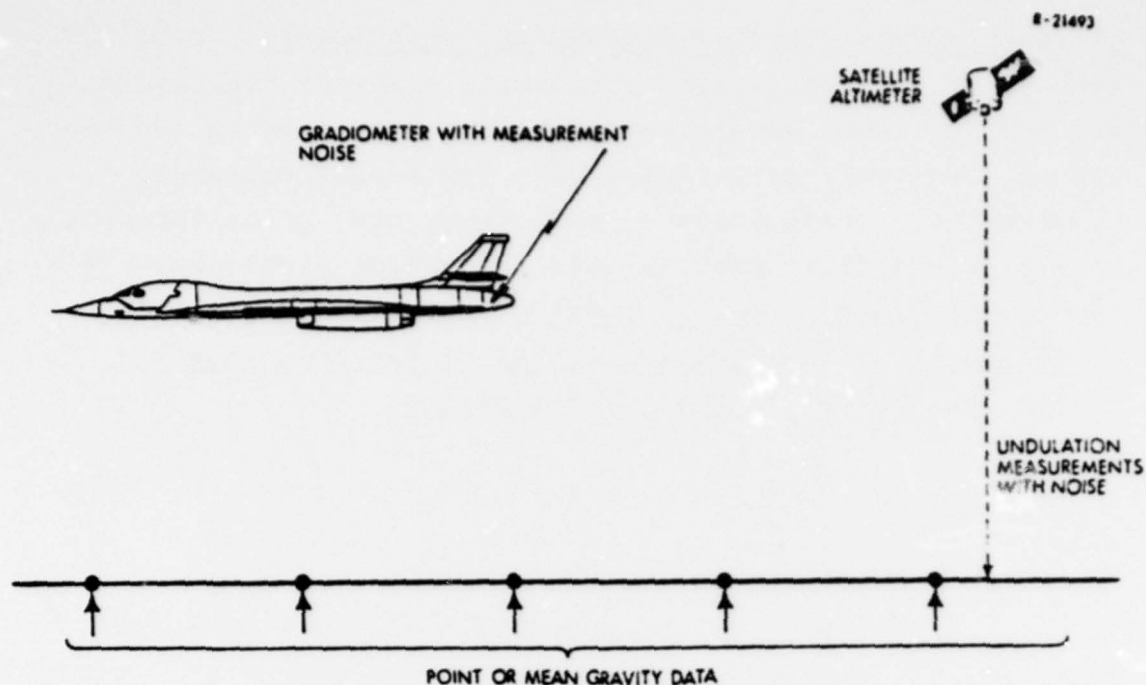


Figure 1.2-1 One-Dimensional, Multisensor Gravity Survey

A new computationally-efficient gravity data processing technique is described which employs finite-dimensional frequency domain techniques. This approach substantially reduces the computer processing requirements for producing minimum variance gravity quantity estimates. This improvement in efficiency is of practical importance because of the severe computational requirements of existing gravity quantity estimation (least-squares collocation) techniques. A typical gravity data processing problem of moderate size (10,000 data points) might require several days of computer time with the existing least-squares collocation methodology. The same problems can be handled in less than a minute with frequency domain methods.

Numerical examples are provided which demonstrate the performance of the frequency domain method on gravity survey problems of the type described above. Used in conjunction

with a new TASC-developed statistical gravity model that is particularly attractive, the method provides a fast, versatile gravity quantity estimation tool.

1.3 TECHNICAL APPROACH

The technique of minimum variance estimation provides the general framework for optimal gravity quantity estimation as discussed in this report. The term least-squares collocation is often applied to this methodology in connection with geophysical applications. This technique is fundamentally statistical in nature, and relies on a statistical model in the form of covariance relationships to provide the connection between the data and the quantity to be estimated, and to provide a characterization of noise in the data. For example, if airborne gravity gradiometry measurements are used to estimate the gravity anomaly at the earth's surface, a covariance matrix must implicitly characterize the physical upward continuation of the gravity disturbance to the aircraft altitude. Other covariance matrices must characterize the quality of any prior knowledge of gravity anomaly in the survey region, as well as the random noise in the gradiometer itself. The least-squares estimation equations specify the operations that must be carried out with these covariance matrices to form optimal (minimum mean-squared error) gravity quantity estimates based on the data. An error covariance analysis based on these equations, and containing matrix operations of similar form, predicts the squared error in the resulting estimates. These relationships are diagrammed in Fig. 1.3-1.

Frequency domain methods provide a substantial reduction in the numerical cost of performing the matrix

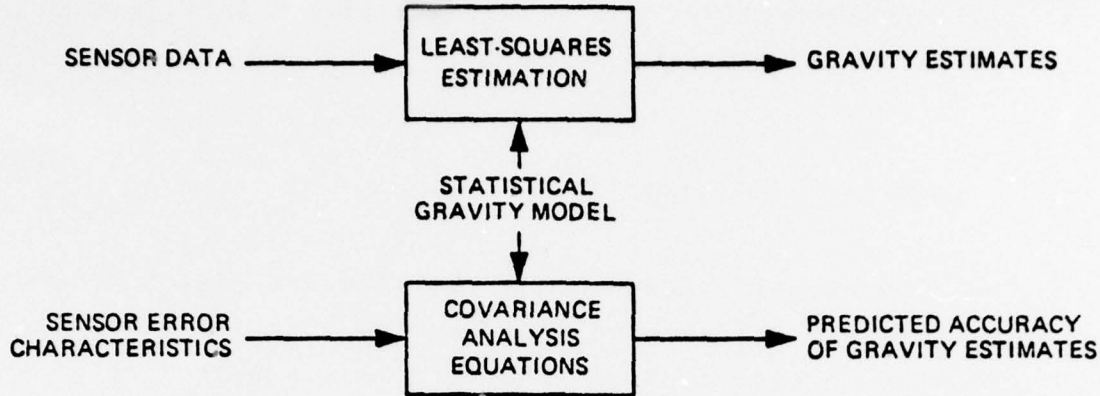


Figure 1.3-1 Least Squares Estimation and Covariance Analysis

operations inherent in the least squares estimation equations (Refs. 12-15). The key to this result is that covariance matrices of a certain general structure become diagonal in the frequency domain. The crucial operations of matrix inversion and matrix multiplication then require substantially fewer computer operations (multiplications, additions, retrievals from storage) than in the full-matrix case. This reduction in computational cost more than compensates for the cost of transformations to and from the frequency domain. The conceptual relationship between the direct application of the least-squares estimation equations and the frequency domain approach is illustrated in Fig. 1.3-2.

The requirements for the applicability of the frequency domain method are simply related to the mathematical structure of the covariance matrices involved. In terms of the gravity quantity estimation problem itself, it is required that the data be available at uniformly spaced points, although interpolated data is acceptable, and that the survey track be long compared to the distance over which the relevant gravity quantity remains highly correlated. These

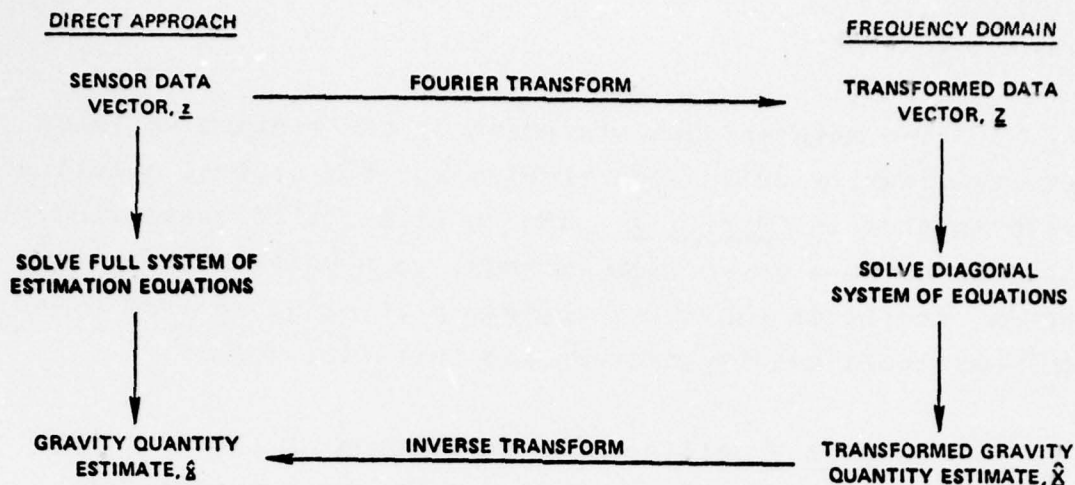


Figure 1.3-2 Relationships Between Direct Least-Squares Estimation and the Frequency Domain Approach

requirements seem reasonable for the gravity survey types considered in this report.

The extension of the techniques of this report to gravity quantity estimation on a two-dimensional survey region seems appropriate under requirements similar to those above. Here the need for uniformly spaced data translates into a requirement for uniform data intervals, measured as spherical angles, along both axes of a two-dimensional grid. Interpolated or averaged data remains a possibility for the two-dimensional problem. Under these conditions, an application of the two-dimensional, finite Fourier transform would lead to a diagonalization of the estimation equations, analogous to the one-dimensional case. Extension of the frequency domain methods of this report offers all of the computational advantages associated with the one-dimensional procedure.

1.4 OVERVIEW

The mathematical statement of the minimum variance gravity quantity estimation problem and its general solution are presented in Chapter 2. The application of these general expressions to a given problem requires specific statistical models, and it is shown how these may be obtained from a new TASC-developed gravity disturbance potential model.

Chapter 3 outlines the derivation of the finite frequency domain estimation method for single-sensor data. A covariance simulation demonstrates the application of the method to estimation of the gravity anomaly using airborne gravity gradiometer data. Further numerical work evaluates the impact of finite track length approximations on the utility of the frequency domain method.

Frequency domain methods for least-squares estimation with multisensor data are considered in Chapter 4. In some important situations with multisensor data the frequency domain equations are no longer diagonal, but retain useful structure. A sequential, one-sensor-at-a-time method is presented which recovers the diagonal structure in these cases. The multisensor frequency domain technique is demonstrated with error covariance analyses for surveys using airborne gradiometry, satellite altimetry, and surface gravimetry in combination for the estimation of the gravity anomaly.

Chapter 5 reviews the results of this report and discusses further applications and extensions of frequency domain techniques in multisensor gravity data processing.

2. LEAST SQUARES ESTIMATION OF GRAVITY QUANTITIES

2.1 STATEMENT OF THE PROBLEM

Measurements, z^1, z^2, \dots, z^N of variables corresponding to N different sensors, which may be, for example, gravity gradiometry, satellite altimetry, or conventional gravimetry are available along one dimensional data grids. These observations contain additive random instrumentation noise. The problem is to compute optimal estimates of a gravity disturbance quantity x , which may typically be the gravity anomaly, vertical deflections, or disturbance potential, at grid points on or above a one-dimensional survey track (Fig. 1.2-1). Note that the data and survey tracks need not all be at one altitude, so that essentially a two-dimensional survey geometry is being considered. The estimates for x are to be optimal with respect to a statistical model which:

- Is consistent with the physical constraints between x and z^1, \dots, z^N (e.g., upward/downward continuation).
- Contains prior statistical knowledge or assumptions concerning x, z^1, \dots, z^N .
- Describes the characteristics of the measurement noise present in the data.

The estimate \hat{x} sought for x is to be optimal in the sense of minimizing the mean squared error $E[(x-\hat{x})^2]$, where $E[\cdot]$ denotes the ensemble expectation operator.

The point sensor "measurements" may themselves be the result of the preprocessing of some raw data. In the

case of airborne gradiometry, for example, the data might be obtained as a sampled moving window average of a continuous instrument measurement. Surface gravimetry data might be the result of interpolating or averaging data from some more complicated survey geometry.

The relationships among the mathematical estimation problem, the underlying physical variables, and the statistical models involved are best described with a concrete example. The example presented here will be followed up in subsequent sections, culminating with a numerical example in Section 3.3.

2.1.1 Example Problem Formulation

It is assumed that a single element of the gravity gradient tensor is to be measured via airborne gradiometry, and that the information gathered is to be used to estimate the gravity anomaly along the aircraft's flight path. The gravity gradient at the aircraft altitude is measured at points along a regular grid. The gravity anomaly is to be estimated at the points of a similar grid on the surface. These quantities are most easily handled in vector form. The gridded values of the gravity anomaly and the observed gradient are denoted*

$$\begin{aligned}\underline{x} &= (x_1, \dots, x_n)^T && \text{(gravity anomalies)} \\ \underline{z} &= (z_1, \dots, z_n)^T && \text{(observed gradients)}\end{aligned}\tag{2.1-1}$$

respectively. For simplicity, it has been assumed that the two sampling grids are of the same lengths and spacing, so that \underline{x} and \underline{z} are of the same dimension.

*The superscript (T) denotes the transpose operation.

The required statistical models for \underline{x} and \underline{z} may be divided into a statistical gravity model, which describes the gravity anomaly and its relationship to the true, or noise-free, value of the anomalous gradient, and a model for measurement noise in the observed values of the anomalous gradient. It is convenient to express these observations as

$$\underline{z} = \underline{y} + \underline{v} \quad (2.1-2)$$

where \underline{y} contains the values of the "true" anomalous gradient, and \underline{v} consists of random measurement noise.

The statistical gravity model consists of the discrete auto- and cross covariance functions

$$\begin{aligned} \phi_{xx}(k) &= E(x_j x_{j+k}) \\ \phi_{yy}(k) &= E(y_j y_{j+k}) \\ \phi_{xy}(k) &= E(x_j y_{j+k}) \end{aligned} \quad (2.1-3)$$

for $1 \leq j, (j+k) \leq n$. The measurement noise \underline{v} is modeled as being statistically uncorrelated with \underline{x} and \underline{y} , with autocorrelation given by

$$\phi_{vv}(k) = E(v_j v_{j+k}) \quad (2.1-4)$$

All three variables \underline{x} , \underline{y} , \underline{z} have zero mean.

The specification of the statistical models completes the definition of the mathematical estimation problem for the example at hand. The specifics of the computation of optimal estimates will be considered in Section 2.2.

2.1.2 The Role of Statistical Models

Apart from the mechanics of computing gravity anomaly estimates, the role of statistical models in the example just presented merits discussion at this point. Perhaps the most important factor in a gravity quantity estimation problem of this type is the set of physical consistency relationships that link the observable variables with those to be estimated. These relationships will be properly accounted for in the estimated process if, and only if, they are embodied in the associated statistical gravity model. For the airborne gradiometry example this means that the operations of upward continuation and differentiation which relate the gravity anomaly and the observed anomalous gradient must be implicit in Eq. 2.1-2. For this reason, the idea of self-consistency in the construction of gravity models, as considered in Refs. 8 and 9, is very important to the estimation process.

The estimation problem described in this section can be extended by introducing uncertain, but nonrandom, parameters into the measurement expression, Eq. 2.1-2:

$$\underline{z} = H\underline{\theta} + \underline{v} + \underline{y} \quad (2.1-5)$$

where $\underline{\theta}$ is a vector of unknown parameters and H is a matrix with compatible dimensions. The term $H\underline{\theta}$ represents "systematic effects" present in the data. This can be useful in modeling effects such as sensor biases or drifts which lead to trends in the data. The estimation of $\underline{\theta}$ and \underline{y} from measurements of the form Eq. 2.1-5 has been considered using the method of least-squares collocation (Refs. 3, 4). This treatment leads to estimation expressions similar to those presented in Section 2.2, which are based on Eq. 2.1-2. The approach to least-squares estimation based on Eq. 2.1-2 is used in this report because it leads more directly to the

frequency domain methodology. The explicit application of frequency domain methods to models using Eq. 2.1-5 would be a useful continuation of the present work.

2.2 LEAST-SQUARES ESTIMATION AND ERROR ANALYSIS

The solution to the least-squares estimation problem is most easily presented in vector-matrix notation. The column vector notation used in the sequel is defined in Table 2.2-1. The ordering of multisensor data within \underline{y} and \underline{z} is left unspecified because it does not have impact on the general estimation expressions presented in this section.

TABLE 2.2-1
VECTOR NOTATION FOR MULTISENSOR ESTIMATION

VECTOR	DEFINITION	DIMENSION
\underline{x}	Gridded values of quantity to be estimated	n
\underline{y}	True values of observed variables (all sensors) at grid points	m
\underline{v}	Random measurement noise	m
\underline{z}	Observed data ($\underline{z} = \underline{y} + \underline{v}$)	m

The information provided by the statistical models associated with the above variables, typically available in the form of Eq. 2.1-3, 2.1-4 is conveniently expressed in covariance matrix form. The $p \times q$ matrix

$$C_{ab} = E(\underline{a} \underline{b}^T) \quad (2.2-1)$$

denotes the covariance matrix of random (zero mean) vectors \underline{a} and \underline{b} of dimension p and q , respectively. The statistical covariance model associated with the estimation problem consists of the matrices C_{xx} , C_{yy} , C_{xy} , C_{vv} , which, together with the assumption that \underline{y} and \underline{v} are independent, yields the data covariance matrix

$$C_{zz} = C_{yy} + C_{vv} \quad (2.2-2)$$

The expressions for minimum variance estimation and error covariance analysis are well known (Refs. 16,17). The optimal estimate for \underline{x} , based on the model provided by Eqs. 2.1-2 through 2.1-4, is

$$\hat{\underline{x}} = C_{xz} C_{zz}^{-1} \underline{z} \quad (2.2-3)$$

This expression utilizes the assumption that \underline{x} and \underline{z} have zero a priori means. If this is not the case, the vectors $\hat{\underline{x}}$ and \underline{z} in Eq. 2.2-3 must be replaced by their respective departures from the means of \underline{x} and \underline{z} . A statistical prediction of the estimation error associated with $\hat{\underline{x}}$ as computed by Eq. 2.2-3 may be obtained as the covariance matrix of the estimation error, $\underline{e} = \underline{x} - \hat{\underline{x}}$. The latter error matrix may be computed from

$$C_{ee} = C_{xx} - C_{xz} C_{zz}^{-1} C_{zx} \quad (2.2-4)$$

Although the matrix C_{ee} gives a complete statistical picture of the errors in $\hat{\underline{x}}$ and their correlations, it is useful to relate the overall estimation error in a given situation to a single quantity. The rms estimation error, σ_e , defined by

$$\sigma_e^2 = \frac{1}{n} E[\underline{e}^T \underline{e}] = \frac{1}{n} \sum_{k=1}^n E[(x_k - \hat{x}_k)^2] \quad (2.2-5)$$

will be used extensively in the sequel. For the one-dimensional gravity survey grid considered in this report, σ_e^2 may be interpreted as the average squared estimation error along the survey track. It is readily calculated from C_{ee} using*

$$\sigma_e^2 = \frac{1}{n} \text{tr}(C_{ee}) \quad (2.2-6)$$

While Eqs. 2.2-3, 2.2-4 provide a very general vehicle for the calculation of optimal gravity estimates, in problems of even moderate size they present computer processing problems that cannot be overlooked. Both expressions contain C_{zz}^{-1} , the inverse of a matrix whose dimension equals the number of data elements, m . The most efficient general algorithms for producing the required inverse (which, for efficiency, would actually involve solving a system of linear equations) call for a number of numerical operations proportional to m^3 . This has a very strong limiting effect on the amount of data for which it is economical to apply Eqs. 2.2-3, and 2.2-4. For example, on a modern, fast computer 15 minutes would be sufficient to calculate the vector $C_{zz}^{-1} \underline{z}$ for $m=1000$, but approximately 10 days would be required for $m=10,000$. Based as much on numerical accuracy problems as on consumption of computer time, a figure of 1000 data elements ($m=1000$) may be taken as a practical upper bound for the successful direct application of Eqs 2.2-3 and 2.2-4.

*The symbol $\text{tr}(C_{ee})$ denotes the trace of the matrix C_{ee} , i.e., the sum of the diagonal elements of C_{ee} .

The airborne gradiometry example of the last section helps to put the numerical processing problem into perspective with the physical availability of data. If gravity gradient data were recorded at 1 nm intervals, then a survey flight of moderate length might yield data at 1000 locations along the survey track. If only one element of the gravity gradient tensor is measured, then, by taking great care with numerical algorithms, Eqs. 2.2-3 and 2.2-4 might be used directly. If, however, more than one of the five independent gradient elements is measured at each location, then Eqs. 2.2-3 and 2.2-4 as they stand are probably not satisfactory because of the computer time requirement alone. This problem is further compounded by the addition of data from any other sensors, or of data from other, parallel survey tracks. The need to efficiently apply Eqs. 2.2-3 and 2.2-4 to gravity estimation problems of this type provides the motivation for the frequency domain approach to computation developed in the sequel.

2.3 STATISTICAL GRAVITY MODELS

The optimal estimation expressions require statistical covariance functions for the gravity disturbance quantities involved. As discussed earlier in the chapter, the choice of the covariance functions used for this purpose must be restricted to those which obey the appropriate physical consistency relations. The construction of gravity disturbance models has been considered by a number of authors (Refs. 7 to 11).

Of the available self-consistent models, those of Refs. 9, 10, and 11 are the only ones that provide covariance expressions for points at different altitudes without requiring analytically intractable or numerically expensive

upward continuation operations. The models of Heller (Ref. 11) and Bellaire (Ref. 10) have the practical advantage that they are simple, and therefore quite tractable. The model used for the purposes of this report is the asymptotic form of the spherical earth "attenuated white noise" (AWN) model developed in Ref. 11. This model is mathematically equivalent to the one derived in Ref. 10 based on "flat earth" geometry. As discussed below, this asymptotic form of the AWN model is somewhat more generally applicable than the "flat earth" derivation of Ref. 10 would suggest, and yet is simpler than the more general spherical earth AWN model.

The geometry of the spherical earth AWN model is illustrated in Fig. 2.3-1. Suppose the disturbance potential on a spherical shell at depth D is taken to be uncorrelated from point to point, i.e., white noise. Then the appropriate upward continuation integral may be solved analytically for the disturbance potential autocovariance, $\phi_{TT}(\psi, r_1, r_2)$ between points at radii r_1 and r_2 separated by a spherical angle ψ . A useful approximation to this autocovariance function may be obtained by taking the limit as the ratio of shell depth to the Earth's radius, and shift angle approach zero. The resulting asymptotic form of the AWN model disturbance potential autocovariance function is

$$\phi_{TT}(t, h_1, h_2) = \frac{4D^2(2D+h_1+h_2)\sigma_T^2}{\left[(2D+h_1+h_2)^2 + t^2\right]^{3/2}} \quad (2.3-1)$$

where t is the shift distance between points and h_1, h_2 are heights above the earth's surface. A disturbance potential model of more general form can be created by superposing versions of Eq. 2.3-1 with differing parameters (σ_T and D).

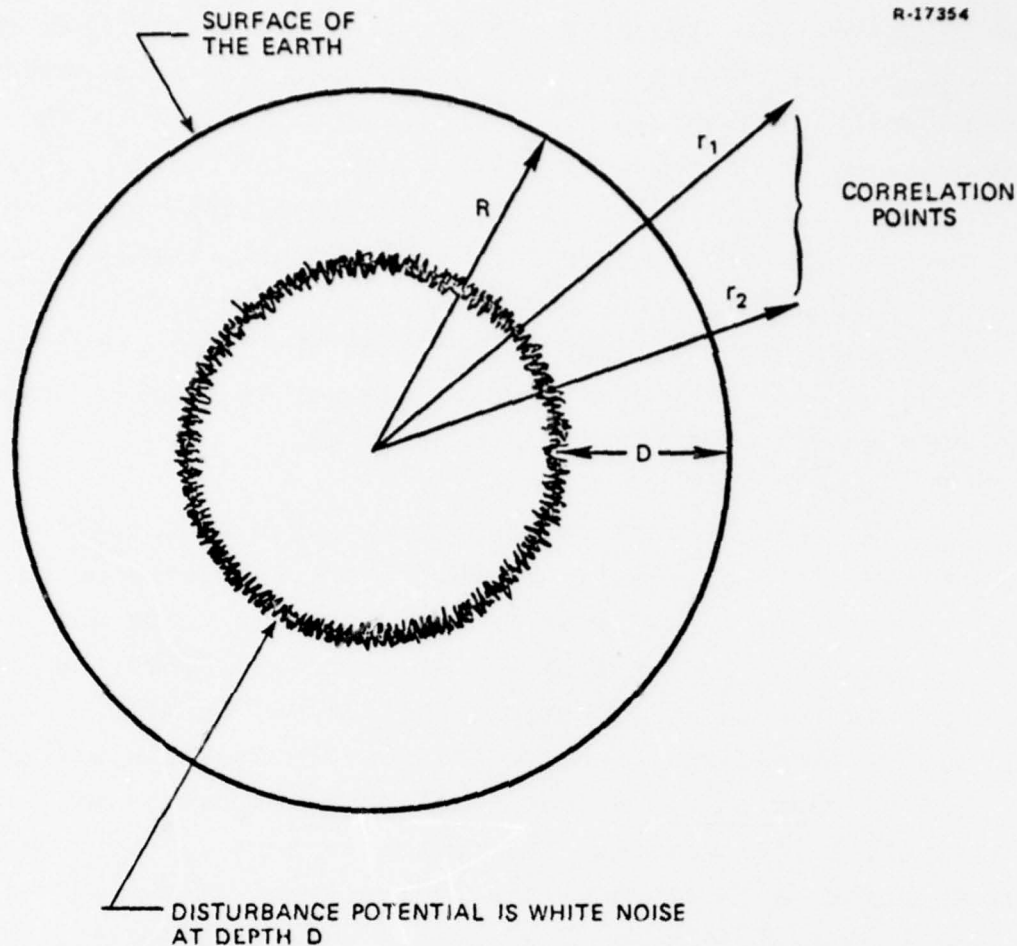


Figure 2.3-1 Geometry of Round Earth,
Attenuated White Noise Model

The result of such a superposition can be viewed as a model based on several white noise shells with differing intensities and depths. The ability of this procedure to represent real data is indicated in Ref. 11, where a "three shell" model has been used to approximate a worldwide gravity anomaly autocovariance function with less than 1% rms error.

It is important to observe that the application of Eq. 2.3-1 is not restricted to situations where flat earth geometry may be expected to be a good physical approximation.

Analysis presented in Ref. 11 shows that Eq. 2.3-1 is a good approximation to its spherical analog for shell depths, D , less than several hundred miles, with no restrictions on altitude above the surface. The reader is referred to Ref. 11 for a derivation and analysis of the asymptotic form of the AWN model, as well as for a demonstration of its capability to fit real data.

Given an expression for the disturbance potential autocovariance function, the required covariance function models for other anomalous gravity quantities may be obtained through simple, mathematical operations. The undulation of the geoid is of interest for gravity survey applications involving satellite altimetry. The necessary statistical model for the undulation, N , may be obtained directly from Eq. 2.3-1 using Brun's formula (Ref. 18):

$$N = \frac{T}{g_0} \quad (2.3-2)$$

where g_0 is the nominal local magnitude of the gravity vector. Covariance models for gravity anomaly, the elements of the gravity disturbance vector, and the elements of the gravity gradient tensor are required in survey applications using gravimetry or gravity gradiometry. These quantities are physically related to the disturbance potential through the appropriate derivative operations (Ref. 18). It follows from the elementary properties of covariance functions (Ref. 19) that self-consistent models for these quantities can be produced by applying corresponding derivative operations to the disturbance potential autocovariance function. These are tabulated in Appendix F of Ref. 11. Expressions for these derivatives can be generated by an automated procedure, such as the IBM FORMAC routine.

The attenuated white noise model of Eq. 2.3-1, together with Eq. 2.3-2 and the capability for automated differentiation, provides a readily accessible, self-consistent statistical gravity model of great flexibility. All of the statistical models for the numerical examples in this report were generated in this way.

3. FREQUENCY DOMAIN ESTIMATION WITH
SINGLE-SENSOR DATA

3.1 THE FREQUENCY DOMAIN ALGORITHM

Frequency domain estimation is a fast computational technique for carrying out least-squares estimation and estimation error analysis. For a broad class of estimation problems it produces essentially the same result as the direct least-squares procedure of Section 2.2, but at a small fraction of the computational cost. This is possible because the transformation to the frequency domain allows the structural regularities already present in the estimation expressions to be put to good use. For the simplest case, the least-squares equations, which are full but highly regular in their usual representation, become diagonal in their frequency domain form. The reduction in cost of carrying out the simplified equations more than compensates for the required transformations to and from the frequency domain. Comparative estimates of numerical processing times (IBM 370/165) for frequency domain and direct estimation are presented in Table 3.1-1. When the number of data points, n , is large, the time required for the direct method is larger by a factor proportional to $n^2/\log n$.

The statistical theory of spectral representation (Refs. 20 - 22) provides elegant motivation for the use of frequency domain estimation methods. This body of mathematical theory is concerned with the statistical characteristics of Fourier-transformed random processes. Let \underline{x} be a random n -vector, and let \underline{X} denote its discrete Fourier transform (DFT), defined as the column vector with the elements *

TABLE 3.1-1
COMPARATIVE COMPUTER PROCESSING TIMES FOR DIRECT, LEAST-SQUARES ESTIMATION AND FREQUENCY DOMAIN ESTIMATION

Number of Data Points	1000	10,000	50,000
Direct Estimation†	14 min	10 days	~3 years
Frequency Domain Estimation	<< 1 sec	1.4 sec	10 sec

$$X(\omega) = \frac{1}{\sqrt{n}} \sum_{k=0}^{n-1} x_{k+1} \exp\left(\frac{2\pi i \omega k}{n}\right) \quad (3.1-1)$$

for $\omega = 0, \dots, n-1$. Suppose that \underline{x} is statistically stationary in the sense that

$$E(x_k x_{k+j}) = \phi_{xx}(j) ; \quad 1 \leq j, (j+k) \leq n$$

An important result of spectral representation theory (Ref. 21) states that the frequency domain elements $X(\omega)$ and $X(\rho)$ are, within an "edge effect" approximation, statistically uncorrelated for $\omega \neq \rho$. A similar result for any pair of random vectors, \underline{x} and \underline{z} , provides for the lack of correlation between the transforms $X(\omega)$ and $Z(\rho)$ with $\omega \neq \rho$. These are the key results which motivate frequency domain estimation techniques.

The application of spectral representation theory to the least-squares estimation problem leads to an algorithm which is a variation on the classic Wiener-Kolmogorov filter (Ref. 23). Let \underline{x} and \underline{z} be defined, following the notation of Section 2.2, as the vector to be estimated and the data

*The letter i denotes the complex number $\sqrt{-1}$.

†Processing times based on use of a direct matrix inversion procedure to solve Eq. 2.2-3.

vector, respectively. The spectral representations of the elements of these vectors, $X(\omega)$ and $Z(\omega)$, can be computed using Eq. 3.1-1. Under regularity conditions corresponding to Eq. 3.1-2, the values of these transforms at any one frequency are uncorrelated with their values at any other frequency. This implies that least-squares estimation of $X(\omega)$ can be carried out based only on the data at the same frequency, $Z(\omega)$. The application of the least-squares equations, Eq. 2.2-3 and 2.2-4, one frequency at a time leads to

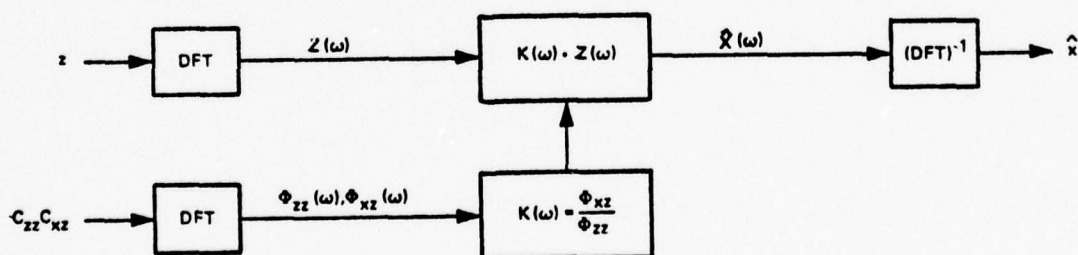
$$\hat{X}(\omega) = \frac{\phi_{XZ}(\omega)}{\phi_{ZZ}(\omega)} Z(\omega) \quad (3.1-3)$$

$$\phi_{ee}(\omega) = \phi_{xx}(\omega) - \frac{\phi_{XZ}(\omega) \phi_{ZX}(\omega)}{\phi_{ZZ}(\omega)} \quad (3.1-4)$$

The quantities $\phi_{xx}(\omega)$, $\phi_{zz}(\omega)$, and $\phi_{xz}(\omega)$ correspond to the appropriate frequency domain variances, and covariances, of $X(\omega)$ and $Z(\omega)$. The expressions in Eq. 3.1-3 and 3.1-4 form the basis of the single-sensor, frequency domain estimation algorithm. The overall procedure is presented in Fig. 3.1-1.

ESTIMATION ALGORITHM

R-34284



ESTIMATION ERROR ANALYSIS

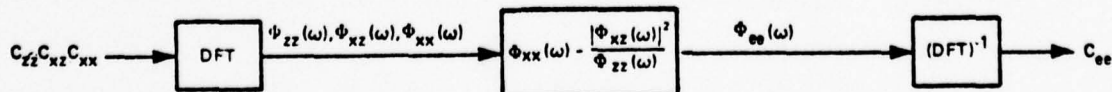


Figure 3.1-1 Single Sensor Frequency Domain Estimation

The requirements for the applicability of the frequency domain estimation procedures are based primarily on the stationarity condition, Eq. 3.1-2. The statistical gravity model of Section 2.3 is of the stationary type, as are all of the models proposed in Refs. 6 - 11. For \underline{x} and \underline{z} based on grids with uniform spacing, and when only single sensor data is used, Eq. 3.1-2 will be satisfied with these models. A more complete set of necessary conditions is presented in Section 3.2.

Computation with the frequency domain estimation method is facilitated by some useful numerical devices. The fast Fourier transform (FFT) algorithm (Refs. 24,25) can be used to efficiently carry out the required transforms and inverse transforms. The use of the FFT accounts for a part of the superior speed of the method. The statistics $\phi_{xx}(\omega)$, $\phi_{zz}(\omega)$, and $\phi_{xz}(\omega)$ are computed as power spectral densities based on the matrices C_{xx} , C_{zz} , and C_{xz} which define the original estimation problem. The mathematical definition for these power spectra is provided in Appendix A (Eq. A-5). Finally, the rms estimation error, σ_e , can be computed without performing the inverse transform of $\lambda_{ee}(\omega)$ by using a form of Parseval's identity (Ref. 25)

$$\sigma_e^2 = \sum_{\omega=0}^{n-1} \phi_{ee}(\omega) \quad (3.1-5)$$

3.2 RELATIONSHIP WITH LEAST-SQUARES ESTIMATION

Generalized Wiener filter theory (Refs. 26, 27) provides a framework for establishing the relationship between direct least-squares estimation and the frequency domain estimation method. This approach reveals the frequency domain method simply as an algebraically transformed version of the

standard least-squares procedure, modified for computational efficiency. One result of this treatment is insight into the asymptotic equivalence of the estimates produced by the direct least-squares and frequency-domain methods. Edge effect approximations cause the estimates computed with the frequency domain method to depart somewhat from the exact, least-squares solution. Under the appropriate conditions the departure from the least-squares estimates becomes arbitrarily small as survey track length is increased. Another important application of the methodology outlined in this section is the development of frequency domain techniques appropriate for multisensor problems, as discussed in Chapter 4.

A block diagram of the generalized Wiener filter process is illustrated in Fig. 3.2-1. This technique is based upon the fact that least-squares estimation may be equivalently carried out under any appropriate transformation. Such a transformation is defined by applying a nonsingular matrix F via

$$\underline{Z} = F\underline{z} \quad , \quad \underline{X} = F\underline{x} \quad (3.2-1)$$

and computing the least-squares estimate of \underline{X} based on \underline{Z} . The matrix F may be complex-valued. It has been assumed for simplicity that \underline{x} and \underline{z} are of the same dimension. The final result is obtained by applying the inverse transformation to the estimate for \underline{X} computed in this way. It can be shown (Ref. 26) that this (unmodified) estimate agrees precisely with the one that would have resulted had no transformation been interposed at all, i.e., the result of Eq. 2.2-3. The objective of this procedure is to select F to reduce the overall cost of computing estimates.

The numerical structure of the least-squares equations under the transformation of Eq. 3.2-1 determines the

computational cost of the procedure. The transformed least-squares estimation and error analysis expressions are (Ref. 27) simply the usual formulas, Eqs. 2.2-3 and 2.2-4, with the transformed statistics*

$$C_{XX} = FC_{xx}F^{\dagger}, \quad C_{ZZ} = FC_{zz}F^{\dagger}, \quad C_{XZ} = FC_{xz}F^{\dagger} \quad (3.2-2)$$

An appropriate transformation can simplify these covariance matrices and the resulting equations considerably. It is well known that the Karhunen-Loeve transformation (KLT) is optimal in the sense that it diagonalizes the least-squares equations (Ref. 28). This produces the greatest reduction in the cost of computing the transformed estimates. Unfortunately, this otherwise ideal transformation is very expensive to compute. Recent design procedures have centered on the use of alternative transformations which combine the desirable diagonalization property with computational efficiency.

The frequency domain estimation procedures of this report are generalized Wiener filtering algorithms employing the discrete Fourier transform. This transformation can be represented by the $n \times n$ matrix (Ref. 25, p. 5)

$$F = [F_{jk}] = \frac{1}{\sqrt{n}} [e^{-2\pi i jk/n}] \quad (3.2-3)$$

where $0 \leq j, k \leq n-1$. Two properties make this transformation attractive:

- The transformed least-squares equations resulting from Eq. 3.2-2 are approximately diagonal for a broad class of statistical models.

*The superscript (+) denotes the complex conjugate, transpose operation.

- The use of the fast Fourier transform algorithm allows the necessary transformations to be carried out with a high degree of efficiency.

Frequency domain estimation techniques thus draw on both statistical theory and the theory of "fast" transforms for their utility. The statistical theory of spectral representation, outlined briefly in the last section, provides for the approximate diagonality of the transformed estimation equations, while the FFT technique makes the transform domain efficiently accessible. The single-sensor version of this algorithm is the discrete Wiener filter described in Section 3.1, and presented in Fig. 3.2-1.

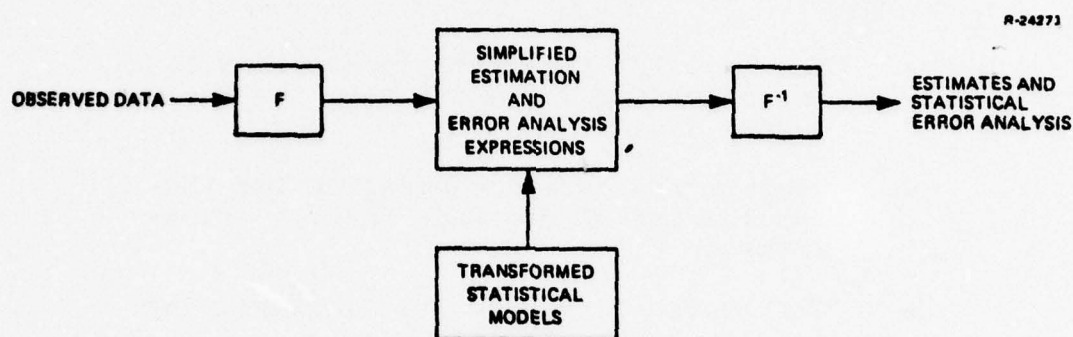


Figure 3.2-1 The Generalized Wiener Filter

The application of the frequency domain estimation method involves neglecting the off-diagonal terms in the transformed covariance matrices of Eq. 3.2-2. These terms correspond to cross covariances which are approximately zero according to the spectral representation theory of Section 3.1. Simplification of the estimation and error analysis expressions by neglecting these small terms is responsible for the substantial savings in computer time associated with the frequency domain approach. The approximations inherent in neglecting off-diagonal terms leads to what have been called "edge effects"

(Ref. 32) in the resulting estimates. A considerable body of matrix theory relates to the analysis of these approximations (Refs. 13, 14, 15 and 35). The analysis briefly outlined in Appendix A shows, for a given estimation problem (of the sort which obeys the restrictions below), that edge effects become arbitrarily small for a survey track of sufficient length. In this sense, the estimates produced using frequency domain techniques are asymptotically equal to the optimal, least-squares estimates. The impact of edge effects on estimation error is investigated numerically in Section 3.4.

The requirements for applicability of the frequency domain techniques of this report arise from three sources:

- The need for regularity conditions to insure strong diagonality in the frequency domain.
- Appropriate data organization for the application of discrete Fourier transforms.
- The suitability of statistical gravity models which are stationary in a Cartesian coordinate system.

Note that this last condition does not restrict the method to "flat-earth" geometry; distance along the curved surface of the earth can be used as the independent variable. Very large surveys can thus be accommodated. A more problem-oriented list of restrictions is as follows:

- Statistical models for the relevant gravity quantities and for measurement noise must be stationary.
- Observations must be taken at uniform spacing (or it must be possible to mathematically place the problem in this format).

- The length of the survey track must be at least several times the longest correlation distance appearing in the statistical models.

3.3 NUMERICAL SIMULATION

An estimation error covariance analysis is described in this section as a numerical demonstration of the frequency domain estimation procedure. The problem considered is the airborne gradiometric survey of gravity anomalies as described in Section 2.1. The rms gravity anomaly estimation error is computed as a function of the survey parameters, including gradiometer accuracy and aircraft altitude, using Eq. 3.1-4. This numerical work is carried out under the following assumptions:

- For simplicity, only a single component of the gravity gradient tensor is observed. The particular component used is the one judged to be most closely related to gravity anomaly.
- The required covariance function models are obtained from the attenuated white noise model described in Section 2.3.
- Gradiometer measurement error is modeled as white noise.
- The observed gravity gradient is the result of a ten second "moving window" average of the gradiometer output.

These assumptions are discussed below.

The measured gravity gradient element is taken to be the along-track derivative of the vertical gravity disturbance, defined by

$$\gamma(t) = \frac{\partial}{\partial t} \delta g(t, h) \quad (3.3-1)$$

where

δg = vertical component of the gravity
disturbance vector

t = distance along survey track, $0 \leq t \leq T$

h = aircraft altitude

This seems a natural choice because of the close relationship between gravity anomaly and vertical gravity disturbance, and because the latter quantity would be determined, within a constant of integration, by a precise measurement of $\gamma(t)$ along the survey track.

The required gravity model for this problem consists of the autocovariance functions for the anomalous gravity gradient at the aircraft altitude and gravity anomaly at the surface, as well as the cross covariance function between these two quantities. These covariance functions are obtained from the attenuated white noise model using automated differentiation as described in Section 2.3.

The modeling of gradiometer measurement error as white noise is consistent with the error models that have been proposed for these instruments (Refs. 30, 31, 32). This model has the physical appeal that it is a good representation for random molecular or electronic error, which is recognized as a limiting error source. Gradiometer measurement accuracy is specified by the rms error, in Eotvos Units (EU), present in the moving window average of the instrument output. The ten second averaging time was chosen to be in agreement with conventional usage in the gradiometer community. Reference 33 contains a thorough treatment of the relationships among white

noise power spectral density, gradiometer averaging time, and reported gradiometer accuracy.

Figure 3.3-1 displays gravity anomaly estimation error as a function of gradiometer accuracy and aircraft altitude. The numerical value of twenty thousand feet was chosen as a representative survey altitude, while curves for surveys on the surface and at forty thousand feet are shown for comparison. The 0-20 EU accuracy regime displayed includes gradiometers considered to be of moderate accuracy, as well as ideal, noise-free gradiometry. Note that the data for this simulation consists of gradiometry only; no initial gravity anomaly "fix" has been assumed. It is recognized that practical gravity surveys would involve some direct measurement of the gravity anomaly. An interesting feature of these results is that they show a significant residual estimation error with a noise-free gradiometer. This can be explained by the fact that the gradiometer, as a differentiating device, cannot measure the bias (constant) portion of the gravity anomaly. For finite track lengths this inability to measure the zero frequency component also extends to the very low frequencies.

The estimation error power spectral density function describes the "frequency response" of the gradiometer as a device for estimating gravity anomaly. As discussed in Section 3.1, the discrete power spectral density $\phi_{ee}(\omega)$, evaluated at wave number ω , can be viewed as the variance of the component of the estimation error at a given frequency. The theory of spectral representation also states that the components of the estimation error at any two different frequencies are statistically uncorrelated. This is consistent with Parseval's identity, Eq. 3.1-5, which is simply the statement that the total mean square estimation error is the sum, across all wave numbers, of $\phi_{ee}(\omega)$. These characteristics

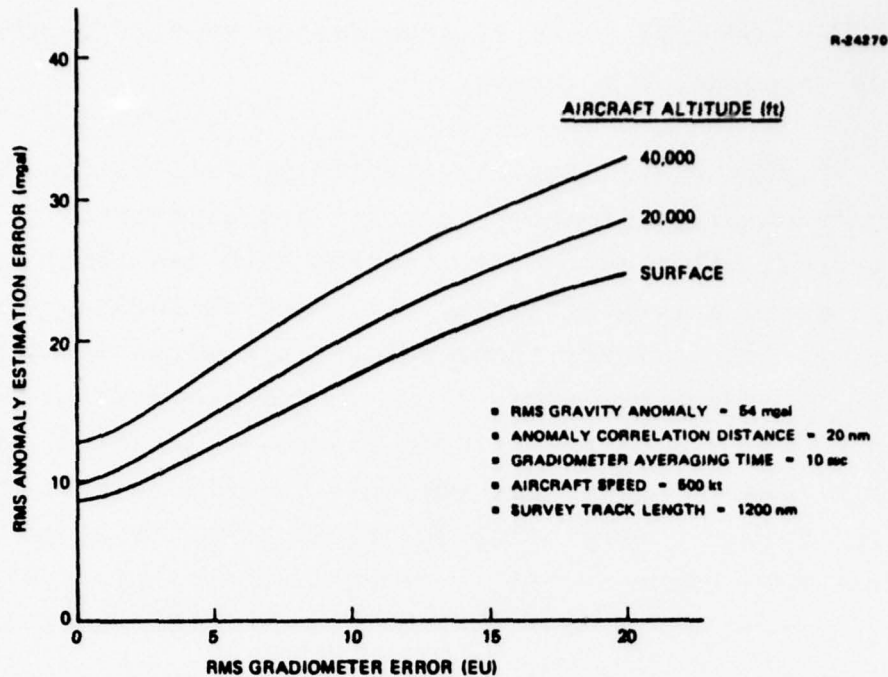


Figure 3.3-1 Projected Gravity Anomaly Estimation Error for an Airborne Survey with Gradiometry Only

make $\phi_{ee}(\omega)$ a useful representation of the estimation error.

Figure 3.3-2 compares the estimation error power spectral density function for 1 and 5 EU gradiometer accuracies with the gravity anomaly power spectral density from which it is derived. As anticipated, the estimation error spectrum is almost entirely confined to the very low wave numbers, reflecting the gradiometer's insensitivity to the bias component of the gravity anomaly. This behavior is seen even more clearly in the spectral coherency function (Ref. 21) defined in the notation of Section 3.1, by

$$\rho^2(\omega) = \frac{|\phi_{xz}(\omega)|^2}{\phi_{xx}(\omega) \phi_{zz}(\omega)} \quad (3.3-2)$$

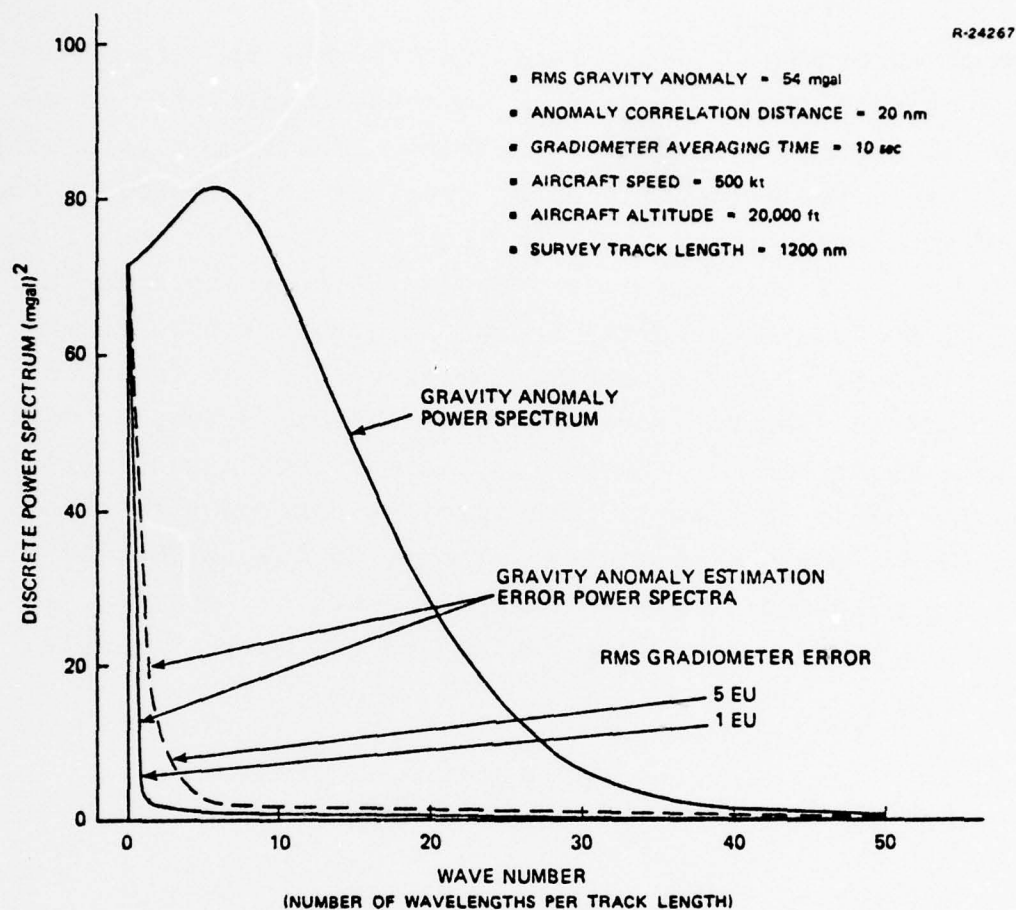


Figure 3.3-2 Power Spectra for Airborne Gradiometry

The usefulness of the spectral coherency function is due to the fact that Eq. 3.1-4 may be rewritten as

$$\phi_{ee}(\omega) = [1 - \rho^2(\omega)] \phi_{xx}(\omega) \quad (3.3-3)$$

Thus the spectral coherency function defines a kind of transfer function between the gravity anomaly power spectrum and the estimation error spectrum of the gravity anomaly. A plot of the gravity-anomaly/gravity-gradient spectral coherency function for rms gradiometer accuracies of 1 and 5 EU is

presented in Fig. 3.3-3. These curves show the effect of increased gradiometer noise as increased "roll-off" at very low and moderately high wave numbers. The impact this roll-off has on the estimation error spectrum is weighted by the gravity anomaly power spectrum (Eq. 3.3-3). The high frequency roll-off has little effect, as is apparent from Fig. 3.3-2, because the gravity anomaly has very little energy in this part of the spectrum. However, the low frequency roll-off in spectral coherency has a strong effect on estimation error because the gravity anomaly has a substantial low frequency component. The spectral coherency function provides a means of assigning changes in the estimation error spectrum directly to changes in sensor response, as weighted by the power spectrum of the estimated variable.

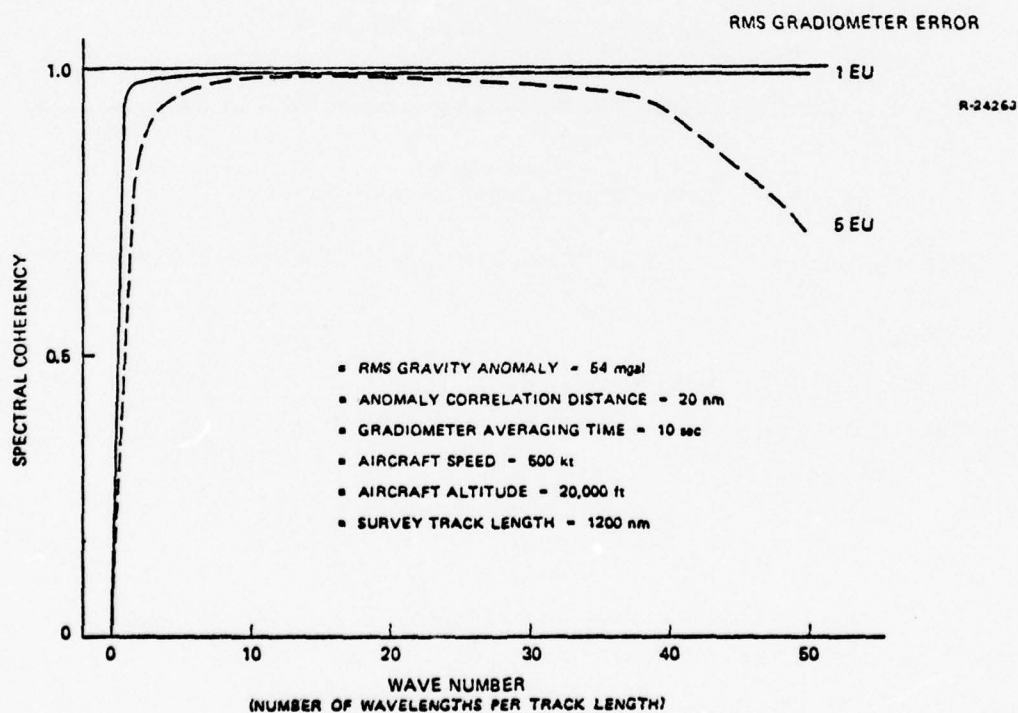


Figure 3.3-3 Gravity-Anomaly/Gravity-Gradient Spectral Coherency Functions for Airborne Gradiometry

3.4 EDGE EFFECT ANALYSIS

For a given estimation problem the gravity quantity estimates computed with frequency domain methods may differ from those obtained via direct least-squares estimation. From the spectral theory viewpoint presented in Section 3.1, this difference is because the Wiener-Kolmogorov filter is optimal only for the case of a survey track of infinite length. Edge effect approximations result when the filter is used for survey tracks of finite length. In the generalized Wiener filter view, edge effects are the result of neglecting off-diagonal terms in the transformed estimation equations. From this perspective, edge effects are the result of a tradeoff of increased estimation error for reduced processing time. Of course, the objective in designing such an estimation procedure is to obtain a very substantial reduction in processing time in exchange for a very small increase in estimation error.

The analysis outlined in Appendix A shows that the increase in rms estimation error due to edge effects becomes arbitrarily small as survey track length is increased. This result provides theoretical justification for the use of frequency domain techniques. The purpose of this section is to present numerical verification of this result for a survey track of finite length.

Numerical evaluation of the portion of estimation error due to edge effects can be obtained by exercising the appropriate error analysis expression. The estimation error covariance matrix associated with an arbitrary linear estimation procedure of the form

$$\hat{\underline{x}} = \underline{G}\underline{z} \quad (3.4-1)$$

is given by (Ref. 17)

$$C_{ee} = C_{xx} - GC_{zx} - C_{xz}G^T + GC_{zz}G^T \quad (3.4-2)$$

The least-squares error covariance expression, Eq. 2.2-4, is a special case of Eq. 3.4-2, when G is the optimal gain matrix of Eq. 2.2-3. With the appropriate choice for G , Eq. 3.4-2 describes the expected squared error associated with frequency domain estimation including edge effect approximations. The proper G matrix is obtained through the procedure used to construct the frequency domain filter as block-diagrammed in Fig. 3.2-1.

In Fig. 3.4-1 the rms gravity anomaly estimation error including edge effects (Eq. 3.4-2) is compared with the optimal estimation error curve from Fig. 3.3-1. Note that the curve labeled "optimal estimation" does not include the edge effect degradation. In the worst case, the increase in estimation error over the optimum is a small fraction of the modeled rms gravity anomaly level. The increased estimation error resulting from edge effects becomes more prominent as gradiometer accuracy is increased. This may be interpreted as a result of the greater demands for precision placed on the estimation procedure by the availability of highly accurate data.

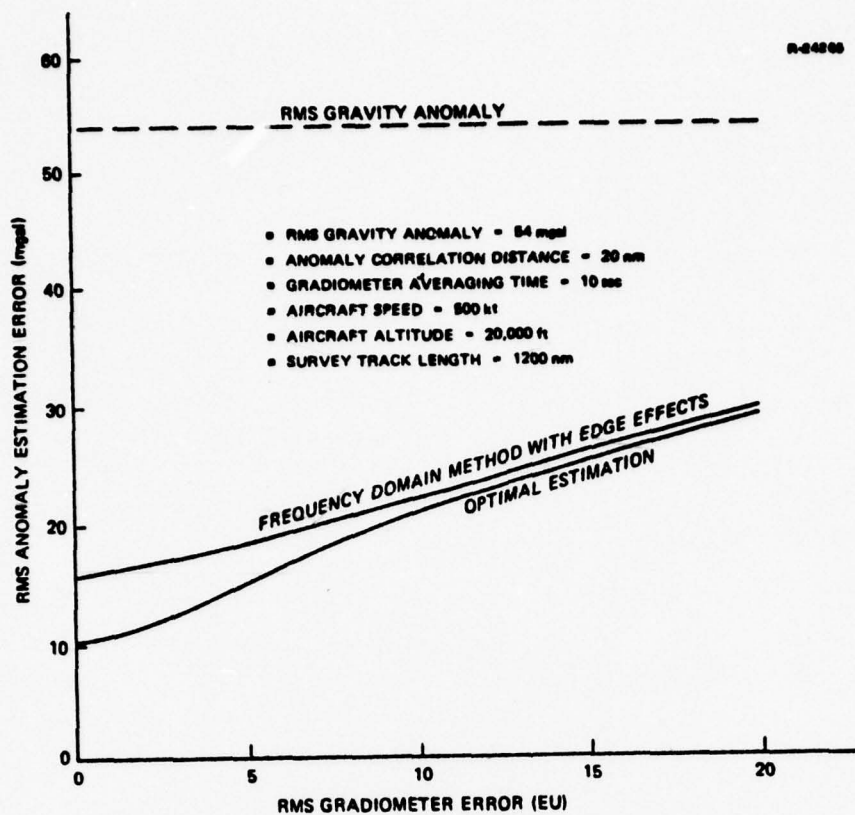


Figure 3.4-1 Estimation Error Sensitivity to Edge Effects

4. MULTISENSOR FREQUENCY DOMAIN ESTIMATION

4.1 PROBLEM FORMULATION

Frequency domain estimation for multisensor problems involves some data structure considerations not present in the single sensor case. Mathematical structure in the least-squares estimation equations appropriate for the use of frequency domain methods depends upon relationships between the data grids for the various sensors. The treatment of multisensor frequency domain estimation is begun in this section by dividing these problems into two classes according to the way the data has been taken. For one class of problems, where the sensor data grids are all "matched" in a certain sense, the applicable frequency domain algorithm does not differ in any fundamental way from the single-sensor method. The necessary extension of the techniques of Chapter 3 is straightforward, with detailed formulas presented in Appendix B.

The second class of problems, characterized by sensor data grids which are "mismatched", is more difficult, and its solution becomes the major theme of the next two sections. Section 4.2 presents a sequential, sensor-by-sensor estimation procedure. While this technique by itself does not result in a faster algorithm, it does provide a useful framework around which to organize multisensor procedures. The derivation of frequency domain statistics suitable for use in multisensor estimation is outlined in Section 4.3. The use of a discrete version of the classical Fourier transform sampling theorem is the major part of this development. The

application of this result in conjunction with the sequential estimation approach provides a solution to the second, more difficult class of multisensor estimation problems.

Throughout this report it is assumed that the data are observed on one-dimensional grids with uniform spacing, or, at least, that the situation appears this way in terms of the mathematics of estimation. In treating multisensor estimation, it is convenient to distinguish between problems where the data grids for the various sensors are matched, and where they are not. In this context, two data grids are matched if they have these characteristics:

- Both grids have uniform measurement point spacing. The point spacing need not agree between grids.
- Both grids have the same number of data points.

This definition clearly includes grids which are physically matched, i.e., those for which the measurement points from different grids overlay one another. It also encompasses those situations where data grids are matched mathematically, perhaps involving a change of scale or a phase shift.

Gravity gradiometry involving the measurement of more than one gradient provides a ready example of the matched grid estimation problem. When a moving-base gradiometer is used to make a series of simultaneous measurements of two or more gradient elements, the data from each of these sensors fall at the same spatial points. The resulting data grids are physically matched.

The use of airborne gradiometry in conjunction with point gravimetry at the surface illustrates the estimation problem with mismatched data grids. Airborne gradiometer measurements are available on a continuous, or nearly continuous, basis. However, surface gravimetry points may be separated by many miles, or many tens of miles. For a survey of the same physical region, the data grids from these two sensors cannot be made compatible. Multisensor surveys with mismatched data grids, such as this one, constitute an important class of estimation problems. Frequency domain techniques for dealing with these problems are developed in the next two sections.

The single-sensor frequency domain methods of Chapter 3 are readily adapted to multisensor problems of the sort with matched data grids. This can be accomplished by treating the observed data as a vector-valued, rather than a scalar, function of distance along the survey track. The generalization in the frequency domain estimation expressions then simply involves the replacement of certain scalar quantities with their vector or matrix analogs. This extension is made explicit in Appendix B. An equivalent estimation procedure, based on sequential techniques, is discussed in the next section.

4.2 SEQUENTIAL, SENSOR-BY-SENSOR ESTIMATION

Sequential data processing, handling data from only one sensor at a time, helps to mitigate the added complexity of multisensor estimation. The sequential estimation and error analysis procedure presented in this section is well known and has found application in many forms (Refs. 17, 29,

35). It should be stressed that the technique explicitly considered here, unlike the recursive Kalman filter algorithm, does not directly reduce computational effort. Its main utility is rather that it reduces the complexity of the estimation and error analysis expressions that must be considered at any one time. In conjunction with frequency domain methodology, this is advantageous because it helps to expose the mathematical structure which accompanies each sensor.

Consider the estimation of an unknown vector \underline{x} using the information contained in two data vectors \underline{u} and \underline{v} . The unknown vector might consist of gravity anomaly values on some survey grid, while \underline{u} and \underline{v} contain the data from two different sensors such as gravity gradiometry and gravimetry. The least-squares estimate for \underline{x} based only on the information in \underline{u} and the accompanying estimation error covariance matrix are, from Eqs. 2.2-3 and 2.2-4:

$$\hat{\underline{x}} = C_{xu} C_{uu}^{-1} \underline{u} \quad (4.2-1)$$

$$C_{ee} = C_{xx} - C_{xu} C_{uu}^{-1} C_{ux} \quad (4.2-2)$$

The results of Eqs. 4.2-1 and 4.2-2 can be updated recursively to account for the additional information provided by \underline{v} . If $\hat{\underline{x}}_u$ and $C_{ee \cdot u}$ are used to denote the results of Eqs. 4.2-1 and 4.2-2, respectively, then the statistical literature (Ref. 35) provides the estimate and error matrix based on both \underline{u} and \underline{v} as

$$\hat{\underline{x}}_{uv} = \hat{\underline{x}}_u + C_{xv \cdot u} C_{vv \cdot u}^{-1} (\underline{v} - C_{vu} C_{uu}^{-1} \underline{u}) \quad (4.2-3)$$

$$C_{ee \cdot uv} = C_{ee \cdot u} - C_{xv \cdot u} C_{vv \cdot u}^{-1} C_{vx \cdot u} \quad (4.2-4)$$

These equations represent another application of Eqs. 2.2-3 and 2.2-4, except that the covariance matrices involved are conditioned on \underline{u} . That is, each covariance matrix is present in its usual context, with its form modified to account for the information in \underline{u} . These conditional covariance matrices are given by the expressions

$$C_{vv \cdot u} = C_{vv} - C_{vu} C_{uu}^{-1} C_{uv} \quad (4.2-5)$$

$$C_{xv \cdot u} = C_{xv} - C_{xu} C_{uu}^{-1} C_{uv} \quad (4.2-6)$$

Note that the single sensor error covariance expression (Eq. 4.2-2) is also the conditional covariance expression for $C_{ee \cdot u}$, as might be expected. Reference 36 discusses the statistical interpretation of covariances conditioned on the data already processed.

The procedure described above extends naturally from two to an arbitrary number of sensors. The use of conditional covariance expressions analogous to Eqs. 4.2-2, 4.2-5 and 4.2-6 provides conditional statistics based on the group of sensors already processed. The substitution of the resulting covariance matrices into the conventional estimation formulas Eqs. 2.2-3 and 2.2-4 yields the estimation and error analysis expressions for incorporating the next sensor. If one chooses to view the vector \underline{u} as containing the data from all the sensors processed up to a given point, with \underline{v} constituting the data from the next sensor to be added, then Eqs. 4.2-3 and 4.2-4 are the general iterative expressions just described.

4.3 SENSOR-BY-SENSOR ESTIMATION IN THE FREQUENCY DOMAIN

Consider the two sensor estimation problem of the last section, where \underline{x} is to be estimated using data contained in vectors \underline{u} and \underline{v} . First assume for simplicity that \underline{x} , \underline{u} , and \underline{v} are all of dimension n . Then the finite Fourier transform of Eq. 3.2-3 may be applied to each of these vectors, producing the transforms

$$\underline{X} = F\underline{x}, \quad \underline{U} = F\underline{u}, \quad \underline{V} = F\underline{v} \quad (4.3-1)$$

According to the generalized Wiener filter theory of Section 3.2, the covariance matrices associated with these transformed quantities may be taken to be diagonal, with diagonal terms corresponding to the appropriate discrete power spectral density. From Section 3.2, these matrices are all of the form*

$$C_{XX} = F C_{xx} F^{\dagger} = \text{diag}(\phi_{xx}(0), \dots, \phi_{xx}(n-1)) \quad (4.3-2)$$

The substitution of the diagonal covariance matrices into the sensor-by-sensor estimation equations, Eqs. 4.2-1 through 4.2-4, yield the set of equivalent scalar frequency domain expressions below.

$$X_u(\omega) = \frac{\phi_{xu}(\omega)}{\phi_{uu}(\omega)} U(\omega) \quad (4.3-3)$$

$$\phi_{ee \cdot u}(\omega) = \phi_{xx}(\omega) - \frac{|\phi_{xu}(\omega)|^2}{\phi_{uu}(\omega)} \quad (4.3-4)$$

*The notation $A = \text{diag}(a_1, \dots, a_n)$ indicates the matrix with elements $A_{ii} = a_i$, $A_{ij} = 0$; $1 \leq i, j \leq n$, $i \neq j$.

$$\hat{X}_{uv}(\omega) = \hat{X}_u(\omega) + \frac{\phi_{xv \cdot u}(\omega)}{\phi_{vv \cdot u}} [V(\omega) - \frac{\phi_{vu}(\omega)}{\phi_{uu}(\omega)} U(\omega)] \quad (4.3-5)$$

$$\phi_{ee \cdot uv}(\omega) = \phi_{ee \cdot u}(\omega) - \frac{|\phi_{xv \cdot u}(\omega)|^2}{\phi_{vv \cdot u}(\omega)} \quad (4.3-6)$$

A similar substitution into the conditional covariance expressions, Eqs. 4.2-5 and 4.2-6 provides

$$\phi_{vv \cdot u}(\omega) = \phi_{vv}(\omega) - \frac{|\phi_{vu}(\omega)|^2}{\phi_{uu}(\omega)} \quad (4.3-7)$$

$$\phi_{xv \cdot u}(\omega) = \phi_{xv}(\omega) - \frac{\phi_{xu}(\omega)\phi_{uv}(\omega)}{\phi_{uu}(\omega)}$$

The use of Eqs. 4.3-3 through 4.3-7 in an integrated, multisensor algorithm is presented in Fig. 4.3-1. The procedure of the figure provides estimates and estimation error analysis based on an arbitrary number of sensors, with the restriction that all of the sensor grids must be of the matched type. This recursive algorithm is mathematically equivalent to the batch procedure of Appendix C.

The recursive algorithm of Fig. 4.3-1 can be extended to many types of problems with mismatched sensor data grids by applying a sampling theorem. This is used to deduce the format of the appropriate frequency domain expressions for use in the sequential procedure of Section 4.2. Let \underline{y} and \underline{u} be vectors of dimension $m \leq n$, representing sensor data sampled on mismatched grids such that $n = rm$, where r is an integer. The implications of this assumption for practical estimation are discussed below. Under these circumstances \underline{y} may be

regarded as a sampling taken from an n -vector \underline{v}^* with an artificial "data grid" matched to that of \underline{u} . The elements of \underline{v} are related to those of \underline{v}^* by

$$v(j) = v^* \left[(j-1)r + 1 \right], \quad j=1, \dots, m \quad (4.3-8)$$

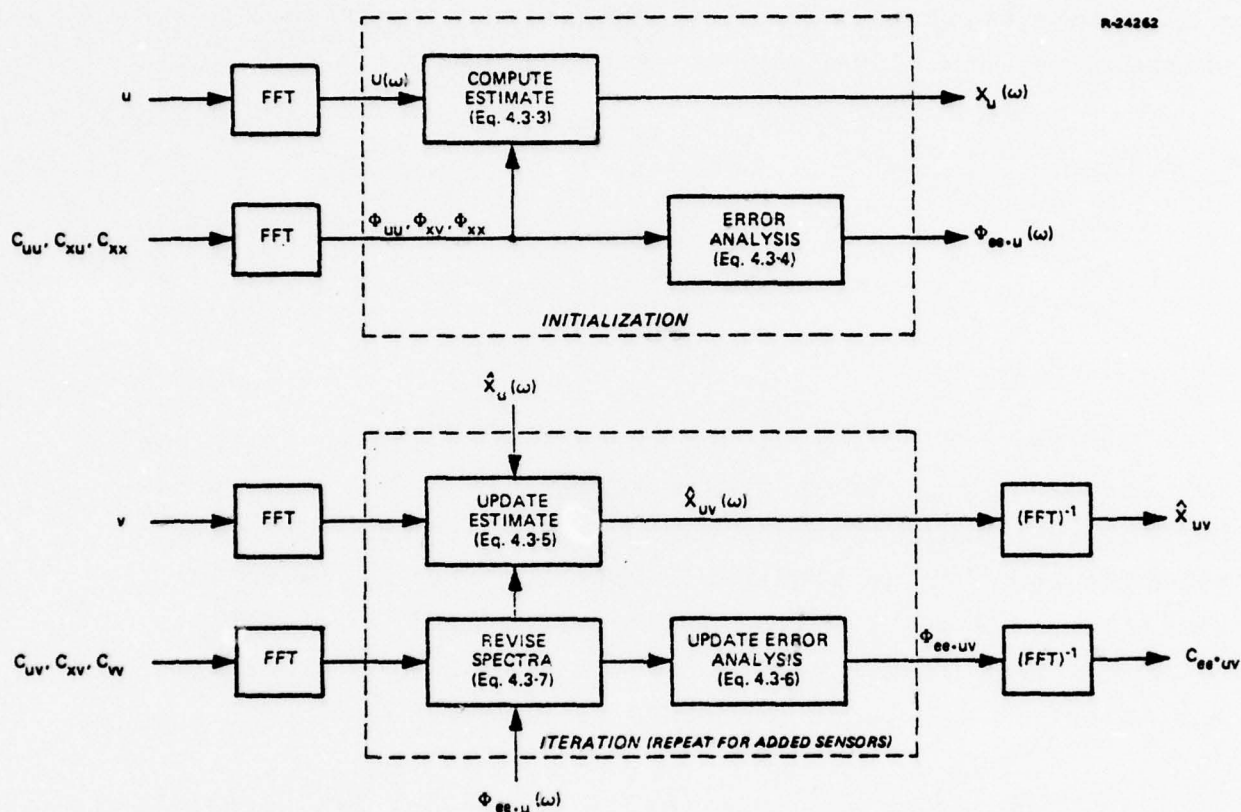


Figure 4.3-1 Sensor-by-Sensor Frequency Domain Estimation

This approach has the advantage, according to the spectral theory of Chapter 3, that the frequency domain covariance matrices involving \underline{v}^* are of known diagonal form. The corresponding matrices for \underline{v} can then be computed directly from the algebraic relationship between \underline{v} and \underline{v}^* in the frequency domain.

The sampling theorem for finite Fourier transforms (Ref. 25) provides the necessary connection between the frequency domain versions of \underline{v} and \underline{v}^* . Letting $V(\omega)$, $\omega=0, \dots, m-1$ and $V^*(\omega)$, $\omega=0, \dots, n-1$ denote these transforms, the sampling theorem provides

$$V(\omega) = \sum_{\rho=0}^{r-1} V^*(\omega+m\rho) \quad (4.3-9)$$

Figure 4.3-2 illustrates the sampling theorem relationship. The algebra of the application of Eq. 4.3-9 to the calculation of the statistics of $V(\omega)$ is treated in Appendix C.

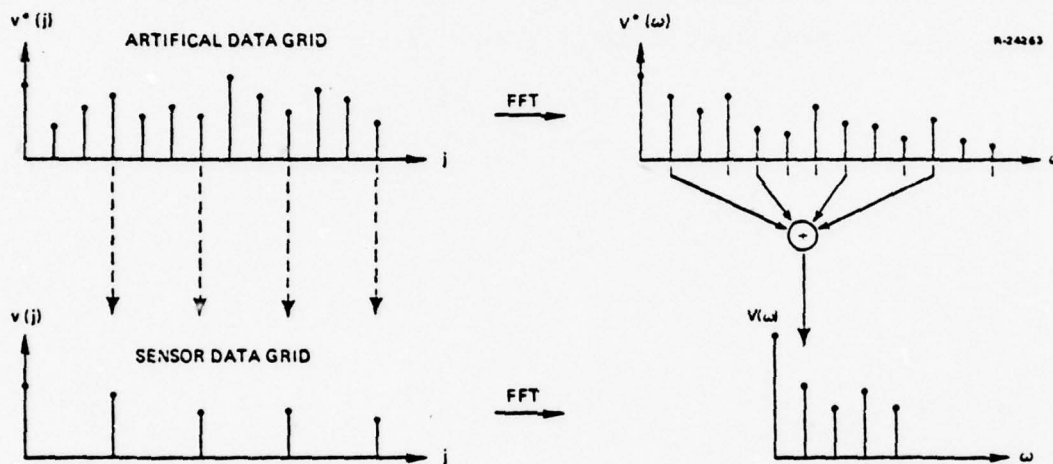


Figure 4.3-2 Sampling Theorem for Finite Transforms

The structure of the multisensor estimation algorithm presented in Fig. 4.3-1 remains appropriate for problems with mismatched data grids. Certain of the spectral equations referred to in the "SENSOR ADDITION" block must be replaced to account for the sampled data analysis discussed above. From Appendix C, the spectral estimation and error analysis formulas analogous to Eqs. 4.3-5 and 4.3-6 are

$$\hat{X}_{uv}(\omega) = \hat{X}_u(\omega) + \phi_{xv*}(\omega) \cdot \phi_{vv \cdot u}^{-1}(\omega \bmod n) \cdot (V - \phi_{vu} \phi_{uu}^{-1} U)(\omega \bmod n) \quad (4.3-10)$$

$$\phi_{ee \cdot uv}(\omega) = \phi_{ee \cdot u}(\omega) - |\phi_{xv* \cdot u}(\omega)|^2 \cdot \phi_{vv \cdot u}^{-1}(\omega \bmod n) \quad (4.3-11)$$

for $\omega=0, \dots, n-1$. The expression $(\omega \bmod m)$ denotes the remainder after integer division by m ,

$$\text{i.e., } (jm+k) \bmod m = k$$

for any integer j and any $0 \leq k \leq m-1$.

The conditional spectral densities which replace Eq. 4.3-7 for the mismatched sensor grid case are given by

$$\phi_{vv \cdot u}(\omega) = \sum_{\rho=0}^{r-1} \left[\phi_{v* v*}(\omega+m\rho) - \frac{|\phi_{uv*}(\omega+m\rho)|^2}{\phi_{uu}(\omega+m\rho)} \right] \quad (4.3-12)$$

for $0 \leq \omega \leq m-1$, and

$$\phi_{xv* \cdot u}(\omega) = \phi_{xv*}(\omega) - \phi_{xu}(\omega) \phi_{uu}^{-1}(\omega) \phi_{uv*}(\omega) \quad (4.3-13)$$

for $0 \leq \omega \leq n-1$. The substitution of Eqs. 4.3-10 and 4.3-11 for Eqs. 4.3-5 and 4.3-6; and the replacement of Eq. 4.3-7 by Eqs. 4.3-12 and 4.3-13 in the procedure of Fig. 4.3-1 allow for the processing of mismatched multisensor data.

The multisensor estimation algorithms described in this section are subject to two restrictions. One of these has been applied to simplify the exposition, the other is more essential. It has been assumed that the vectors \underline{x} and \underline{u} are of the same dimension. This is equivalent to assuming that these quantities have been sampled on matched grids, which serves to simplify the exposition. This restriction may

be removed by applying the sampling theorem approach for mismatched grids which has just been described. A second, more basic restriction on the algorithm is the assumption, in the mismatched data grid case, that the ratio of the amounts of data corresponding to any two sensor grids (i.e. the number r in the analysis above) is an integer. In many problems of interest this restriction can be met through an appropriate arrangement of the input data. For example, when a data "mismatch" results from discretizing an essentially continuous measurement, such as airborne gradiometry, pre-processing may be applied to alter the effective sampling rate. This may be accomplished with no information loss by smoothing with a moving window averager, and then sampling at a carefully chosen increased rate. The new sampling rate may be chosen so that the data mismatch ratio, r , is an integer. Frequency domain techniques are then directly applicable. With suitable structuring of the input data, the computational efficiency associated with frequency domain methodology is available over a wide range of multisensor estimation problems.

4.4 MULTISENSOR NUMERICAL SIMULATION

The results of numerical simulations with the multisensor frequency domain estimation procedure are presented in this section to demonstrate the applicability of the method. These results consist of frequency domain estimation error analyses of two- and three-sensor simulated gravity anomaly surveys. Simulated data sources for the two-sensor survey consist of airborne gradiometry and surface gravimetry. The three-sensor survey is formed by the addition of satellite altimetry. The relevant survey geometry for these simulations is depicted in Fig. 1.2-1.

Apart from the use of multisensor techniques, the methodology applied in this section is much the same as that described in Section 3.3. The statistical models and assumptions associated with the simulation of airborne gradiometry are identical with those of that section. Similar use is made of the attenuated white noise model in the automated generation of the self-consistent disturbance gravity models required in the simulation. This procedure has also been described in Section 2.3.

Surface gravimetry is modeled as a series of point gravity anomaly measurements parameterized by the (uniform) spacing between observation points. A nominal rms gravimetry accuracy of 1 mgal is assumed throughout. Gravimetry errors are assumed to be uncorrelated between observation points.

Satellite radar altimetry observations are simulated as noisy measurements of the undulation of the geoid beneath the satellite's orbit. The separation between successive undulation measurements is parameterized by the altimeter pulse repetition rate and the satellite orbital velocity. An orbital velocity of 8 km/sec is assumed throughout. Altimeter accuracy, as reflected in the rms accuracy of the geoid height determination, is a parameter in the simulation.

The results of the gradiometric/gravimetric survey simulation are presented in Fig. 4.4-1. An interesting feature of this figure is the reduction in gravity anomaly estimation error resulting from the introduction of relatively few gravimetry observations. The spectral analysis of gradiometer response presented in Section 3.3 has shown that most of the estimation error after a survey with a gradiometer alone is at the bias, or very low frequency, level. Gravimetry data complements gradiometry very well by providing measurements sensitive to the bias component in the gravity anomaly.

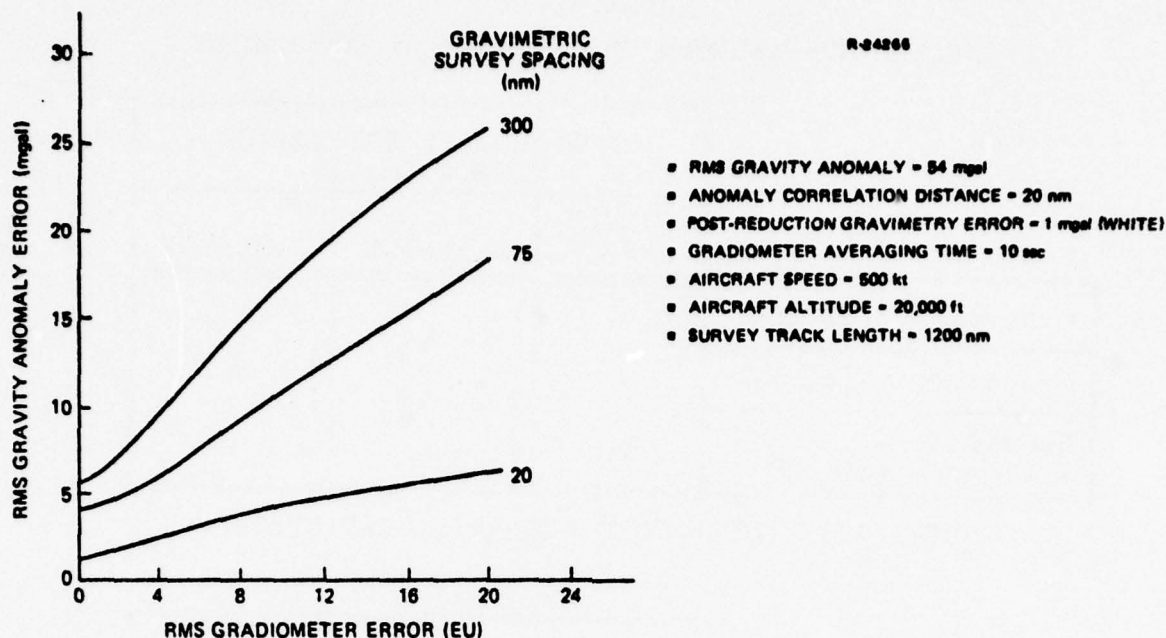


Figure 4.4-1 Projected Gravity Anomaly Estimation Error for a Combined Gradiometric/Gravimetric Survey

The projected gravity anomaly estimation error resulting from two- and three-sensor surveys involving gravimetry, gradiometry, and satellite altimetry in various combinations are shown in Table 4.4-1. The two sections of this table contrast the quality of the estimates that can be obtained using a high quality gradiometer (1 EU) with those obtainable using a gradiometer of lesser accuracy (10 EU).

It is recognized that the rms estimation errors presented in Table 4.4-1 are well in excess of current gravity mapping needs (Ref. 38). These results indicate that gradiometry data from a single, one-dimensional track is not adequate for high precision gravity anomaly estimation. The addition of multiple, parallel data tracks over the survey area should produce considerable improvement in gradiometer-based gravity estimates.

TABLE 4.4-1
PROJECTED MULTISENSOR GRAVITY SURVEY ACCURACIES

	RMS ANOMALY ESTIMATION ERROR (mgal)		
	SINGLE SENSOR	2-SENSOR	3-SENSOR
Gravimetry (75 nm)	42	} 11 16	} 9.3
Gradiometry (10 EU)	21		
Satellite Altimetry (30 cm)	20		

SURVEY WITH MODERATELY ACCURATE GRADIOMETER

	RMS ANOMALY ESTIMATION ERROR (mgal)		
	SINGLE SENSOR	2-SENSOR	3-SENSOR
Gravimetry (75 nm)	42	} 4.3 7.2	} 2.8
Gradiometry (1 EU)	10		
Satellite Altimetry (30 cm)	20		

SURVEY WITH HIGHLY ACCURATE GRADIOMETER

- ONE-DIMENSIONAL SURVEY GEOMETRY
- RMS GRAVITY ANOMALY = 54 mgal
- ANOMALY CORRELATION DISTANCE = 20 nm
- POST-REDUCTION GRAVIMETRY ERROR = 1 mgal (WHITE)
- GRADIOMETER AVERAGING TIME = 10 sec
- AIRCRAFT SPEED = 500 kt
- AIRCRAFT ALTITUDE = 20,000 ft
- SATELLITE ALTIMETER DATA RATE = 10/sec
- SURVEY TRACK LENGTH = 1200 nm

5. CONCLUSIONS AND RECOMMENDATIONS

This report describes the development of new, computationally-efficient techniques for processing multi-sensor gravity data. These procedures apply modern frequency domain signal processing methodology to existing statistical least-squares gravity estimation techniques. The general statistical least-squares approach to gravity quantity estimation:

- Produces theoretically optimum gravity quantity estimates
- Applies to a very general class of gravity sensors and survey types
- Contains a "built-in" capability for statistical estimation error analysis
- Requires self-consistent statistical gravity models.

The conventional least-squares procedure has the disadvantage that numerical processing requirements place important limits on its practical utility. A direct implementation of the least-squares equations leads to computer processing requirements, as well as susceptibility to numerical inaccuracy, that sharply restrict problem size. However, the new procedure largely eliminates these practical difficulties through the introduction of computationally efficient methods.

The frequency domain estimation techniques described in this report are designed to substantially reduce the computer processing requirements of the statistical least-squares

procedure for a wide variety of gravity applications. This technique is based upon the transformation of the least-squares equations into a form advantageous for computation. The overall cost of the resulting procedure is proportional to the cost of a fast Fourier transform (FFT) of the input data. As a result, the computer burden imposed by the frequency domain method is less by orders of magnitude than that of the equivalent direct least-squares procedure.

The efficiency of the frequency domain method is based on the exploitation of the mathematical structure ordinarily present in gravity quantity estimation problems. Requirements for the applicability of the method, based on preserving appropriate structure in the estimation equations, are:

- Regularly gridded data. Data may be preprocessed by averaging or interpolation.
- Stationary statistical gravity models.
- Long gravity survey track length compared to the relevant gravity quantity correlation distances.

The class of problems considered in this report has been limited to estimation along and above a one-dimensional survey track. It is anticipated that the frequency domain technique can be extended for use with two-dimensional survey regions under requirements similar to those above.

Numerical simulations have been carried out to demonstrate the performance of the method. Numerical results include:

- Estimation error analyses for gravity anomaly surveys with one, two, and three sensors.
- Preliminary analyses of the spectral response characteristic of airborne gravity gradiometry.
- Investigation of estimation error sensitivity to frequency domain edge effect approximations.
- Verification of estimated computer processing times for the frequency domain method.

The results presented in this report represent a first step in the application of modern frequency domain signal processing methodology to the processing of gravity data. A number of areas suggest themselves as being worthy of future investigation:

- Development of frequency domain methods suitable for the estimation of gravity on a two-dimensional surface.
- Investigation of frequency domain data compression techniques. The results obtained with frequency domain least squares methods suggest a similar approach to the efficient compression of gravity data.
- Investigation of edge-effect compensation procedures. Numerical results on estimation error sensitivity to the effects of finite track length (Section 3.4) suggests the use of modified frequency domain techniques for some problems.
- Development of spectral sensor response characterization techniques appropriate for multisensor applications. Sensor response comparisons, analysis of sensor information overlap, and multisensor trade-off studies should benefit from an extension of the coherency function idea applied to gradiometry in Section 3.4.

APPENDIX A

ASYMPTOTIC OPTIMALITY OF FINITE,
FREQUENCY DOMAIN ESTIMATION

This appendix presents a brief analysis of the asymptotic optimality property of the finite, frequency domain estimation methods developed in this report. Under appropriate regularity conditions, it is shown that the rms estimation error associated with the frequency domain algorithm converges to the optimum as the survey track length is increased. This analysis, which does not appear to be available in the open literature, provides explicit, theoretical justification for the use of frequency domain procedures in connection with finite estimation problems. The estimation of gravimetric quantities from data is such a problem.

For the problems considered in this report, the covariance matrices appearing in the estimation equations belong to a class of matrices known as Toeplitz forms (Ref. 37). An $n \times n$ matrix C is a Toeplitz matrix if there is some function

$$\phi(\ell), \quad -(n-1) \leq \ell \leq (n-1) \quad (A-1)$$

for which the (j,k) th element of C may be written

$$C_{jk} = \phi(k-j), \quad 1 \leq j, k \leq n \quad (A-2)$$

The covariance matrices associated with weakly stationary random sequences are Toeplitz forms with $\phi(\ell)$ defined by the appropriate autocovariance or cross covariance function. The set of requirements imposed at the end of Section 3.2 assures that the vectors \underline{x} and \underline{z} (in the notation of the body of this

report) can be regarded as finite sections from weakly stationary random sequences.

A major step in the analysis of frequency domain methods is to show that the frequency domain representation of any Toeplitz matrix becomes "asymptotically equivalent" to a diagonal matrix in the limit as n is increased without bound. The idea of asymptotic equivalence used here has previously been employed in the analysis of the limiting behavior of matrix sequences (Ref. 14). This sort of special equivalence definition is valuable because the element by element limit of the matrices of interest here is not, in general, diagonal. Thus, straight-forward limiting analysis cannot produce the necessary diagonal estimation equations.

Following Eq. 3.2-2, the frequency domain representation of an $n \times n$ matrix C is defined by

$$\tilde{C} = FCF^T \quad (A-3)$$

where F is the finite Fourier transform matrix of Eq. 3.2-3. The limiting behavior of $\tilde{C} = \tilde{C}(n)$, with elements defined by Eqs. A-2 and A-3, will be considered as n increases without bound. The sequence of matrices $\{\tilde{C}(n), n=1,2,\dots\}$ will be compared to a sequence of diagonal matrices $\{\tilde{D}(n), n=1,2,\dots\}$. Let the "continued" function $\phi_c(\ell)$, $-(n-1) \leq \ell \leq n-1$ be defined by

$$\phi_c(k) = \begin{cases} \phi(k) & , k=0 \\ \phi(k) + \phi(n-k) & , k \neq 0 \end{cases} \quad (A-4)$$

The discrete power spectral density of the matrix C can now be defined as

$$\phi(\omega) = \frac{1}{n} \sum_{k=0}^{n-1} e^{\frac{-2\pi i \omega k}{n}} \phi_c(k) \quad (A-5)$$

for $\omega = 0, \dots, n-1$. The matrix $\tilde{D}(n)$ is defined by

$$\tilde{D}(n) = n \cdot \text{diag} [\phi(0), \dots, \phi(n-1)] \quad (A-6)$$

The asymptotic equivalence result described in Ref. 14 can be stated as follows

The matrices $\tilde{C}(n)$ and $\tilde{D}(n)$ are asymptotically equivalent in the sense that

$$\lim_{n \rightarrow \infty} \frac{1}{n} \sum_{\text{all } j, k} [\tilde{C}_{jk}(n) - \tilde{D}_{jk}(n)]^2 = 0 \quad (A-7)$$

This is a statement that the average squared difference between $\tilde{C}(n)$ and $\tilde{D}(n)$ vanishes in the limit as n increases without bound.

The asymptotic optimality of the finite, frequency domain estimation procedure is established by examining the limiting forms of the appropriate expressions for rms estimation error. According to the results of Section 3.2, the frequency domain estimation error covariance matrix for the optimal, least-squares procedure is

$$C_{EE} = C_{XX} - C_{XZ} C_{ZZ}^{-1} C_{ZX} \quad (A-8)$$

From Parseval's identity, Eq. 3.1-5, the rms estimation error for the optimal procedure is given by

$$\sigma_e^2 = \frac{1}{n} \text{tr}(C_{EE}) \quad (\text{A-9})$$

The frequency domain covariance matrices of Eq. (A-6) are defined by Eq. 3.2-2. From Section 3.4, the estimation error covariance associated with the finite, frequency domain procedure is

$$C'_{EE} = C_{XX} - GC_{ZX} - C_{XZ}G^T + GC_{ZZ}G^T \quad (\text{A-10})$$

where G is the diagonal gain matrix

$$G = \text{diag} \left(\frac{\phi_{XZ}(0)}{\phi_{ZZ}(0)}, \dots, \frac{\phi_{XZ}(n-1)}{\phi_{ZZ}(n-1)} \right) \quad (\text{A-11})$$

Corresponding to Eq. A-9, the rms estimation error accompanying the finite, frequency domain procedure is

$$\sigma_{e'}^2 = \frac{1}{n} \text{tr}(C'_{EE}) \quad (\text{A-12})$$

Because Eqs. A-8 and A-9 correspond to the optimal estimate, it follows that $\sigma_{e'} \geq \sigma_e$. The main result of this appendix is to show that $\sigma_{e'}$ converges to the optimal rms error:

$$\lim_{n \rightarrow \infty} (\sigma_{e'}^2 - \sigma_e^2) = 0 \quad (\text{A-13})$$

Because n corresponds to a number of data points taken a fixed distance apart, Eq. A-13 refers to a limit as the survey track length is increased without bound.

The analysis which establishes Eq. A-13 is outlined as follows:

- First, it is observed that Eq. A-8 is a special case of Eq. A-10, with gain G_0 given by

$$G_0 = C_{XZ} C_{ZZ}^{-1} \quad (A-11)$$

- Under the appropriate regularity conditions, the preceding analysis shows that the matrices C_{XZ} and C_{ZZ} are asymptotically equivalent to

$$D_{XZ} = \text{diag} [\phi_{XZ}(0), \dots, \phi_{XZ}(n-1)]$$

and

$$D_{ZZ} = \text{diag} [\phi_{ZZ}(0), \dots, \phi_{ZZ}(n-1)]$$

respectively.

- By applying the theorems of Ref. 14 on the inverse and product of asymptotically equivalent matrices, it follows that the gain matrices G and G_0 are asymptotically equivalent. This leads to the conclusions that C'_{EE} and C_{EE} are asymptotically equivalent.
- It can be shown directly from Eq. A-5 that the asymptotic equivalence of C'_{EE} and C_{EE} implies that Eq. A-10 holds.

While the explicit expressions presented in this appendix are for the single-sensor case only, the asymptotic optimality result of Eq. A-13 holds for the multisensor algorithm as well. The analysis for the multisensor case is entirely analogous to that presented here; the difference is primarily one of complexity.

APPENDIX B

MULTISENSOR, DISCRETE WIENER FILTERING

When multisensor data is available, the procedure of Chapter 4 leads to a frequency domain algorithm for gravity quantity estimation that incorporates the data on a sequential, one-sensor-at-a-time basis. In the special case that all the data are available on "matched" grids, as defined in Chapter 4, the resulting multisensor algorithm can be simplified into a single, multidimensional, Wiener filtering procedure. The resulting estimation and estimation error analysis expressions are simply vector-matrix versions of the single-sensor expressions, Eqs. 3.1-3 and 3.1-4. The purpose of this appendix is to provide an explicit presentation of these expressions.

It is useful to arrange the multisensor input data as a sequence of vector-valued measurements. Let the measurement from the j th sensor at the k th grid point be denoted z_k^j , where $1 \leq j \leq N$ and $1 \leq k \leq n$. Because the various sensor data grids are assumed to be matched, these data may be arranged in a single, vector-valued sequence

$$\underline{z}_k = (z_k^1, \dots, z_k^N)^T \quad (B-1)$$

for $k = 1, \dots, n$. The gravity quantity to be estimated is denoted, as before, by the sequence x_k , $k = 1, \dots, n$. The scalar sequence x_k has the finite Fourier transform $X(\omega)$, $\omega = 0, \dots, n-1$, defined by Eq. 3.1-1. Similarly, the vector-valued sequence \underline{z}_k has the finite Fourier transform

$$\mathbf{Z}(\omega) = [\mathbf{Z}^1(\omega), \dots, \mathbf{Z}^N(\omega)^T] \quad (\text{B-2})$$

for $\omega = 0, \dots, n-1$, defined in terms of the scalar transform of each of its elements.

Matrix-valued power spectral densities are required. The power spectrum of \mathbf{z}_k is the sequence of $N \times N$ matrices denoted by $\Lambda_{\mathbf{ZZ}}(\omega)$, $\omega = 0, \dots, n-1$. The $(\ell, m)^{\text{th}}$ element of $\Lambda_{\mathbf{ZZ}}(\omega)$ is the cross power spectral density between $\mathbf{z}^\ell(\omega)$ and $\mathbf{z}^m(\omega)$. More specifically, if $\phi_{\ell m}(k)$ denotes the cross covariance function

$$\phi_{\ell m}(k) = E(\mathbf{z}_j^\ell \mathbf{z}_{j+k}^m) \quad (\text{B-3})$$

for $1 \leq j, (j+k) \leq n$, then $\phi_{\ell m}(\omega)$, defined according to Eq. A-5 as the discrete power spectral density of $\phi_{\ell m}(k)$, is the $(\ell, m)^{\text{th}}$ element of $\Lambda_{\mathbf{ZZ}}$. The $N \times 1$ cross spectral matrix $\Lambda_{\mathbf{xZ}}(\omega)$, $\omega = 0, \dots, n-1$, is defined in the analogous element-by-element fashion. As in the body of this report, the scalar sequence $\phi_{\mathbf{xx}}(\omega)$, $\omega = 0, \dots, n-1$, denotes the power spectral density of \mathbf{x}_k , defined according to Eq. A-5.

The appropriate estimation expression is now simply stated as

$$\hat{\mathbf{X}}(\omega) = \Lambda_{\mathbf{xZ}}(\omega) \Lambda_{\mathbf{ZZ}}^{-1} \mathbf{Z}(\omega) \quad (\text{B-4})$$

for $\omega = 0, \dots, n-1$. The corresponding expression for the estimation error power spectral density is given by

$$\phi_{\text{ee}}(\omega) = \phi_{\mathbf{xx}}(\omega) - \Lambda_{\mathbf{xZ}}(\omega) \Lambda_{\mathbf{ZZ}}^{-1}(\omega) \Lambda_{\mathbf{ZX}}(\omega) \quad (\text{B-5})$$

Note that the matrix inversions indicated in Eq. B-4 and B-5 are of dimension equal to the number of sensors, N .

Through a still more detailed treatment it is possible to write down expressions of greater generality than Eqs. B-4 and B-5. For example, these expressions may be extended to the case where x_k and \underline{z}_k are on mismatched grids. Generalizations of this type may be obtained using the techniques of Chapter 4.

APPENDIX C

DERIVATION OF FREQUENCY DOMAIN STATISTICS USING THE SAMPLING THEOREM

The sampling theorem for finite Fourier transforms is a useful vehicle for the calculation of statistics for multisensor data on grids which are "mismatched" in the sense of Chapter 4. Frequency domain autocovariances and cross covariances involving data on mismatched grids are required in the development of the estimation procedures of Chapter 4. This appendix outlines the use of the sampling theorem in deriving the appropriate expressions.

In the notation of Chapter 4, let \underline{u} and \underline{v} denote data vectors, corresponding to different sensors, of dimension n and m , respectively. The information in \underline{u} and \underline{v} is to be used to compute an estimate of the n -vector \underline{x} . It is assumed that the data which comprise \underline{u} and \underline{v} are available on mismatched grids, with $n > m$. An estimate for \underline{x} is to be computed using the frequency domain version of the sensor-sequential estimation expressions, Eqs. 4.2-1 through 4.2-6. These expressions require all six of the frequency domain covariance matrices associated with the transforms \underline{X} , \underline{U} , and \underline{V} i.e., C_{XX} , C_{XU} , C_{UU} , C_{VX} , C_{VU} , and C_{VV} . Because \underline{x} and \underline{u} are of compatible dimension, the first three of the covariance matrices listed above are known to be well-approximated by diagonal forms (see Eq. 4.3-2). The use of the sampling theorem makes it possible to deduce similar expressions for the covariances that involve the "mismatched" data, \underline{v} .

The elements of \underline{y} are to be viewed as a sampling of an expanded data vector of dimension n , \underline{v}^* . It is assumed that $n = rm$, where r is an integer. The elements of \underline{y} in terms of those of \underline{v}^* are defined by Eq. 4.3-8. The result of the discrete sampling theorem, relating the elements of the m - and n -dimensional transforms \underline{y} and \underline{v}^* , is given by Eq. 4.3-9. This relationship can be expressed in vector-matrix notation as

$$\underline{y} = S \underline{v}^* \quad (C-1)$$

where S is the matrix

$$S = (\underbrace{I_m \quad I_m \quad \dots \quad I_m}_{r \text{ blocks}}) \quad (C-2)$$

The notation I_m indicates the $m \times m$ identity matrix.

The vector \underline{v}^* has been constructed to be statistically stationary, and to be of dimension compatible with \underline{x} and \underline{u} . It follows from the asymptotic analysis discussed in Section 3.2 and detailed in Appendix A, that the covariance matrices C_{V^*U} , C_{V^*X} , and $C_{V^*V^*}$ may be taken to be diagonal. The diagonal of each of these matrices is the power spectral density with the matching subscript, e.g.,

$$C_{V^*U} = \text{diag}(\phi_{v^*u}(0), \dots, \phi_{v^*u}(n-1)) \quad (C-3)$$

The required covariance matrices involving \underline{y} may now be obtained by applying Eqs. C-1 and C-2 to the corresponding diagonal matrices involving \underline{v}^* . The appropriate relations are

$$\begin{aligned}
 C_{VU} &= SC_{V*U} \\
 C_{VX} &= SC_{V*U} \\
 C_{VV} &= SC_{V*V}S^T
 \end{aligned}
 \tag{C-4}$$

The resulting frequency domain covariance matrices are highly structured forms that can be exploited in the estimation equations. This is exemplified by the diagonal-block form

$$C_{VU} = \begin{pmatrix} \phi_{V*U}(0) & \phi_{V*U}(m) & \dots & \phi_{V*U}(n-m) \\ \vdots & \vdots & \vdots & \vdots \\ \phi_{V*U}(m-1) & \phi_{V*U}(2m-1) & \dots & \phi_{V*U}(n-1) \end{pmatrix}
 \tag{C-5}$$

The substitution of the covariance matrices of Eq. C-4, worked out in a form analogous to Eq. C-5, into Eqs. 4.2-3 through 4.2-6 leads to the estimation equations for data on mismatched grids, Eqs. 4.3-10 through 4.3-13.

REFERENCES

1. Gentry, D.C. and Nash, R.A., Jr., "A Statistical Algorithm for Computing Vertical Deflections Gravimetrically," J. Geophys. Res., Vol. 77, 1972, pp. 4912-4919.
2. Rose, R.C. and Nash, R.A., Jr. "Direct Recovery of Vertical Deflections Using an Inertial Navigator," paper presented at the Fall Annual Meeting, American Geophysical Union, San Francisco, California, December 7-10, 1970. (Also see IEEE Trans. Geosci. Electron., Vol. 10, No. 2, 1972, pp. 85-92.)
3. Moritz, H., "A General Theory of Gravity Processing," Report No. 122, Dept. of Geod. Sci., Ohio State Univ., Columbus, Ohio, 1969.
4. Moritz, H., "Least Squares Estimation in Physical Geodesy," Report No. 130, Dept. of Geod. Sci., Ohio State Univ., Columbus, Ohio, 1970.
5. Rapp, R.H., "Numerical Results from the Combination of Gravimetric and Satellite Data Using the Principles of Least Squares Collocation," Report No. 200, Dept. of Geod. Sci., Ohio State Univ., Columbus, Ohio, 1973.
6. Shaw, L., Paul, I. and Henrikson, P., "Statistical Models for the Vertical Deflection from Gravity Anomaly Models," J. Geophys. Res., Vol. 74, 1969, pp. 4259-4265.
7. Kasper, J.F., Jr., "A Second-Order Gravity Anomaly Model," J. Geophys. Res., Vol. 76, 1971, pp. 7844-7849.
8. Jordan, S.K., "Self-Consistent Statistical Models for the Gravity Anomaly, Vertical Deflections, and Undulation of the Geoid," J. Geophys. Res., Vol. 77, 1972, pp. 3660-3670.
9. Tscherning, C.C. and Rapp, R.H., "Closed Covariance Expressions for Gravity Anomalies, Geoid Undulations, and Deflections of the Vertical Implied by Anomaly Degree Variance Models," Report No. 208, Dept. of Geod. Sci., Ohio State Univ., Columbus, Ohio, 1974.

REFERENCES (Continued)

10. Bellaire, R.G., "Statistics of the Geodetic Uncertainties Aloft," American Geophysical Union Fall Annual Meeting, San Francisco, California, December 1971.
11. Heller, W.G., "Self-Consistent Statistical Geodetic and Geophysical Error Models for Land-Based ICBMs," The Analytic Sciences Corp., Report No. TR-573-1, December 1975.
12. Pratt, W.K., "Generalized Wiener Filter Computation Techniques," IEEE Trans. on Computers, Vol. C-21, July 1972, pp. 636-641.
13. Gray, R.M., "On the Asymptotic Eigenvalue Distribution of Toeplitz Matrices," IEEE Trans. Inform. Theory, Vol. IT-18, November 1972, pp. 725-730.
14. Gray, R.M., "Toeplitz and Circulant Matrices: A Review," Technical Report No. 6502-1, Stanford Electronics Laboratories, Stanford, California, June 1971.
15. Baxter, G., "An Asymptotic Result for the Finite Predictor," Math. Scand., Vol. 10, 1962, pp. 137-144.
16. Bryson, A. and Ho, Y.C., Applied Optimal Control, Blaisdell, Waltham, Mass., 1969, pp. 348-364.
17. Gelb, A. (ed.), Applied Optimal Estimation, M.I.T. Press, Cambridge, Mass., 1974.
18. Heiskanen, W.A. and Moritz, H., Physical Geodesy, Freeman, San Francisco, 1967.
19. Parzen, E., Stochastic Processes, pp. 78-87, Holden-Day, San Francisco, 1962.
20. Gikhman, I.I., and Skorokhod, A.V., Introduction to the Theory of Random Processes, Saunders, Philadelphia, 1965.
21. Hannan, E.J., Multiple Time Series, Wiley, New York, 1970.
22. Yaglom, A.M., An Introduction to the Theory of Stationary Random Functions, Prentice-Hall, Englewood Cliffs, New Jersey, 1962.

REFERENCES (Continued)

23. Sage, A.P. and Melsa, J.L., Estimation Theory with Applications to Communications and Control, McGraw-Hill, New York, 1971, pp. 303-315.
24. Cooley, J.W. and Tukey, J.W., "An Algorithm for the Machine Calculation of Complex Fourier Series," Math. of Comp., Vol. 19, 1965, pp. 297-301.
25. Cooley, J.W., Lewis, P.A.W., and Welch, P.D., "The Fast Fourier Transform and Its Applications," Report No. RC-1743, IBM Watson Research Center, Yorktown Heights, New York, 1967.
26. Pearl, J., "Basis-Restricted Transformations and Performance Measures for Spectral Representation," IEEE Trans. Inform. Theory, Vol. IT-17, November 1971, pp. 751-752.
27. Pratt, W.K., "Generalized Wiener Filter Computation Techniques," IEEE Trans. on Computers, Vol. C-21, July 1972, pp. 636-641.
28. Ahmed, N., Natarajan, T. and Rao, K.R., "Discrete Cosine Transform," IEEE Trans. on Computers, Vol. C-23, January 1974, pp. 90-93.
29. Anderson, T.W., The Statistical Analysis of Time Series, Wiley, New York, 1971.
30. Forward, R.L. "Review of Artificial Satellite Gravity Gradiometer Techniques for Geodesy," Hughes Research Laboratories, Research Report 469, May 1973.
31. Trageser, M.B., "Gravity Gradiometer Status Report," Charles Stark Draper Laboratory, Report C-3935, June 1973.
32. Metzger, E.H. "Rotating Accelerometer Gravity Gradiometer Review," Annual Gravity Gradiometer Review Conference, USAF Academy, Colorado, February 1976.
33. Heller, W.G., "Gradiometer-Aided Inertial Navigation," The Analytic Sciences Corp., Report No. TR-312-5, April 1975, Rev. August 1976.

REFERENCES (Continued)

34. Whittle, P., "The Analysis of Multiple Stationary Time Series," J.R. Statist. Soc. B., Vol. 15, 1953, pp. 125-139.
35. Moritz, H., "Stepwise and Sequential Collocation," Report No. 203, Dept. of Geod. Sci., Ohio State Univ., Columbus, Ohio. 1973.
36. Anderson, T.W., An Introduction to Multivariate Statistical Analysis, Wiley, New York, 1958.
37. Grenander, U. and G. Szego, Toeplitz Forms and Their Applications, Univ. of Calif. Press, Berkeley, Calif., 1958.
38. "Development of a Launch Region Gravity Model for Minuteman (U)," Geodynamics Corporation Report No. CDR-0115 (FR3705)-1, March 1970. (SECRET)